Ann. Rev. Fluid Mech. 1985. 17:151–89

AERODYNAMICS OF SPORTS BALLS

Rabindra D. Mehta[1]

Aerodynamics Research Branch, NASA Ames Research Center, Moffett Field, California 94035

1. INTRODUCTION

Aerodynamics plays a prominent role in almost every sport in which a ball is either struck or thrown through the air. The main interest is in the fact that the ball can be made to deviate from its initial straight path, resulting in a curved flight path. The actual flight path attained by the ball is, to some extent, under the control of the person striking or releasing it. It is particularly fascinating that not all the parameters that affect the flight of a ball are under human influence. Lateral deflection in flight (variously known as *swing*, *swerve*, or *curve*) is well recognized in cricket, baseball, golf, and tennis. In most of these sports, the swing is obtained by spinning the ball about an axis perpendicular to the line of flight, which gives rise to what is commonly known as the *Magnus effect*.

It was this very effect that first inspired scientists to comment on the flight of sports balls. Newton (1672), at the advanced age of 23, had noted how the flight of a tennis ball was affected by spin, and he gave this profound explanation: "For, a circular as well as a progressive motion . . . , its parts on that side, where the motions conspire, must press and beat the contiguous air more violently than on the other, and there excite a reluctancy and reaction of the air proportionably greater." Some 70 years later, in 1742, Robins showed that a transverse aerodynamic force could be detected on a rotating sphere. However, Euler completely rejected this possibility in 1777 (see Barkla & Auchterlonie 1971). The association of this effect with the name of Magnus was due to Rayleigh (1877), who, in his paper on the irregular flight of a tennis ball, credited him with the first "true explanation" of the effect. Magnus had found that a rotating cylinder

[1] Present address: Department of Aeronautics and Astronautics, Joint Institute for Aeronautics and Acoustics, Stanford University, Stanford, California 94305.

0066–4189/85/0115–0151$02.00

moved sideways when mounted perpendicular to the airflow. Rayleigh also gave a simple analysis for a "frictionless fluid," which showed that the side force was proportional to the free-stream velocity and the rotational speed of the cylinder. Tait (1890, 1891, 1893) used these results to try to explain the forces on a golf ball in flight by observing the trajectory and time of flight. This was all before the introduction of the boundary-layer concept by Prandtl in 1904. Since then, the Magnus effect has been attributed to asymmetric boundary-layer separation. The effect of spin is to delay separation on the retreating side and to enhance it on the advancing side. Clearly, this would only occur at postcritical Reynolds numbers ($Re = Ud/\nu$, where U is the speed of the ball or the flowspeed in a wind tunnel, d is the ball diameter, and ν is the air kinematic viscosity), when transition has occurred on both sides. A smooth sphere rotating slowly can experience a negative Magnus force at precritical Reynolds numbers, when transition occurs first on the advancing side.

Most of the scientific work on sports ball aerodynamics has been experimental in nature and has concentrated on three sports balls: the cricket ball, baseball, and golf ball. Details of these three balls, together with typical operating conditions, are given in Figure 1.

The main aim in cricket and baseball is to deliberately curve the ball through the air in order to deceive the batsman or batter. However, the tools and techniques employed in the two sports are somewhat different, which results in the application of slightly different aerodynamic principles. An interesting comparison of the two sports is given by Brancazio (1983). In golf, on the other hand, the main aim generally is to obtain the maximum distance in flight, which implies maximizing the lift-to-drag ratio. In this article, the more significant research performed on each of the three balls is reviewed in turn, with emphasis on experimental results as well as the techniques used to obtain them. While many research papers and articles were consulted in preparing this review, only those that have made relevant and significant contributions to the subject have been cited. For an overview of the physics of many ball games, see Daish (1972).

2. CRICKET BALL AERODYNAMICS

2.1 *Basic Principles*

The actual construction of a cricket ball and the principle by which the faster bowlers swing the ball is somewhat unique to cricket. A cricket ball has six rows of prominent stitching, with typically 60–80 stitches in each row (primary seam). The stitches lie along the equator holding the two leather hemispheres together. The better quality cricket balls are in fact made out of four pieces of leather, so that each hemisphere has a line of internal stitching forming the "secondary seam." The two secondary seams,

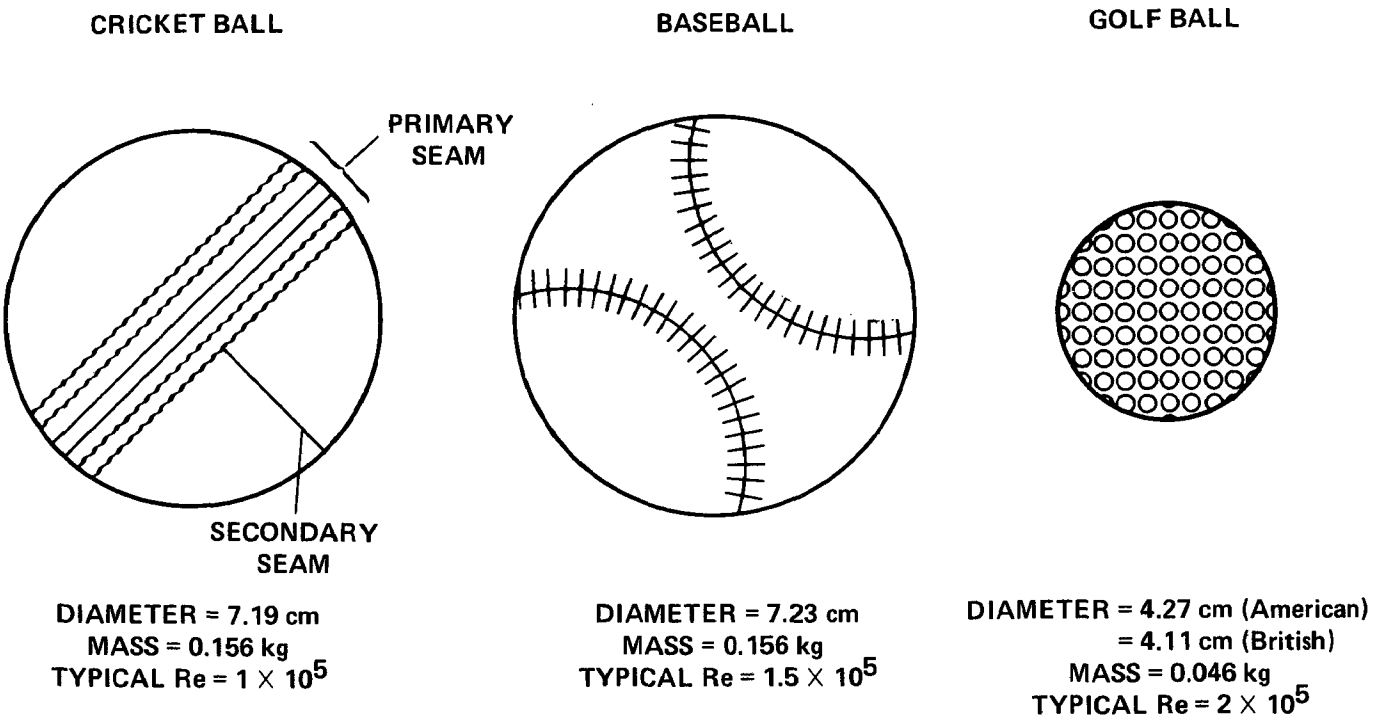

Figure 1 Typical ball dimensions and operating conditions.

primarily designed to strengthen the ball structure, are traditionally set at right angles to each other (Figure 1).

Fast bowlers in cricket make the ball swing by a judicious use of the primary seam. The ball is released with the seam at a small angle to the airflow. Under the right conditions, the seam trips the laminar boundary layer into turbulence on one side of the ball. This turbulent boundary layer, by virtue of its increased energy, separates relatively late compared to the boundary layer on the nonseam side, which separates in a laminar state. Figure 2 shows a cricket ball held stationary in a wind tunnel with the seam set at an incidence angle $\alpha = 40°$ to the airflow. Smoke was injected into the separated region behind the ball, where it was entrained right up to the separation points. The boundary layer on the lower surface has been tripped by the seam into turbulence, evidenced by the chaotic nature of the smoke edge just downstream of the separation point. On the upper surface a smooth, clean edge confirms that the separating boundary layer was in a laminar state. The laminar boundary layer on the upper surface has separated relatively early, at a point which makes an angle θ with the horizontal of about 90°, whereas the turbulent boundary layer on the lower surface separates at $\theta = 120°$. This asymmetry is further confirmed by the upward deflection of the wake flow.

The asymmetric boundary-layer separation results in an asymmetric pressure distribution that produces the side force responsible for the swing. In practice, some spin is also imparted to the ball, but about an axis perpendicular to the seam plane (i.e. along the seam) so that the asymmetry is maintained. A prominent seam obviously helps the transition process, whereas a smooth and polished surface on the nonseam side helps to maintain a laminar boundary layer. For this reason bowlers in cricket normally keep one hemisphere of the ball highly polished, whereas the other hemisphere is allowed to roughen, during the course of play. While it is legal to polish the ball using natural substances such as sweat or saliva, it is not legal to scuff or mark the cricket ball deliberately.

The basic principles behind cricket ball swing have been understood by scientists for years, and the first published discussion is that due to Lyttleton (1957). More recently, Mehta & Wood (1980) discussed the whole subject of cricket ball swing in detail. The two detailed experimental investigations on cricket ball swing are by Barton (1982) and Bentley et al. (1982); the latter is covered briefly in Mehta et al. (1983).

2.2 *Static Tests*

In static tests the cricket ball is held stationary in an airstream and the continuous forces measured, either directly or through integration of the surface pressure distributions.

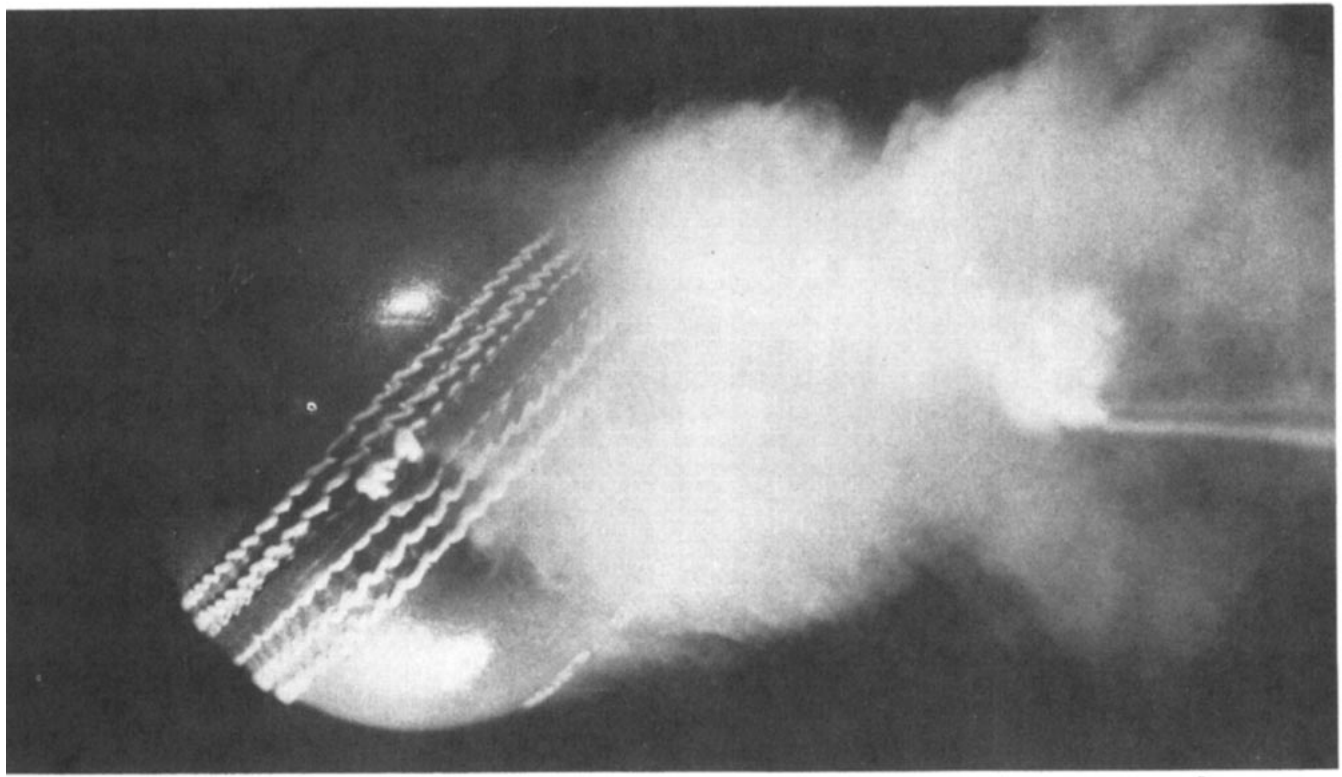

Figure 2 Smoke photograph of flow over a cricket ball. Flow is from left to right. Seam angle = 40°, flowspeed = 17 m s^{-1}, Re = 0.85 × 10^5 (Mehta et al. 1983).

Detailed pressure distributions along the equator of a ball supplied with 24 pressure tappings were measured by Bentley et al. (1982). The pressure tappings were installed in the horizontal plane, perpendicular to the seam plane. Figure 3 shows the measured pressures on the ball mounted in a wind tunnel at $\alpha = 20°$. The measurements on the seam side of the ball are represented by those shown on the right-hand side in Figure 3. At low values of Re or U, the pressure distributions on the two hemispheres are equal and symmetrical, so there would be no side force. At $U = 25$ m s^{-1}, the pressure dip on the right-hand face of the ball is clearly lower than that on the left-hand face. This would result in the ball swinging toward the right. The maximum pressure difference between the two sides occurs at $U =$ 29 m s^{-1}, when presumably the boundary layer on the seam side is fully turbulent while that on the nonseam side is still laminar. Even at the highest flowspeed achieved in this test ($U = 36.5$ m s^{-1}), the asymmetry in pressure distributions is still clearly indicated, although the pressure difference is reduced. The actual (critical) flowspeeds at which the asymmetry appears or disappears were found to be a function of the seam angle, surface roughness, and free-stream turbulence—in practice it also depends on the spin rate of the ball. In general, though, a roughness height of the same order as the boundary-layer thickness is required for the successful transition of a

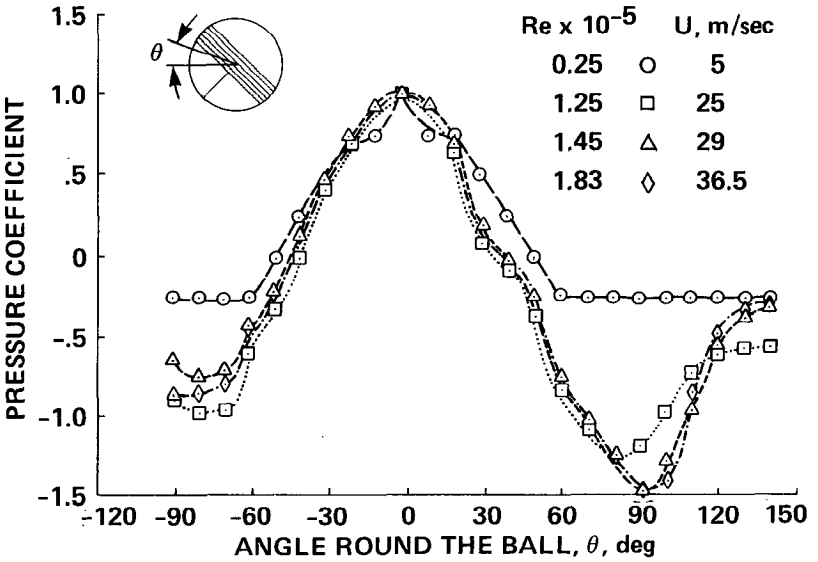

Figure 3 Pressure distributions on a cricket ball held at an incidence angle of 20° (Mehta et al. 1983).

laminar boundary layer into turbulence. Typically, the primary seam height is about 1 mm, and the laminar boundary-layer thickness at, say, $\theta = 20°$ is less than 0.5 mm. In terms of Reynolds number, Graham (1969) suggested that the value of Re based on roughness height should be at least 900. For a cricket ball seam, this corresponds to $U \sim 14$ m s^{-1}. Note that the magnitude of the suction peaks in Figure 3 (~ -1.5) often exceeds that given by potential-flow theory for spheres (-1.25). Bentley et al. (1982) attributed this to the higher induced velocities due to "tip vortices" produced on lifting bodies of finite span.

Barton (1982) measured side forces on cricket balls by using a compound pendulum system where the ball was allowed to swing transversely. The side force can be evaluated once the transverse deflection is measured. Figure 4 shows some of Barton's results obtained using this technique. Except for the ball that had been used in a cricket match for 40 overs (240

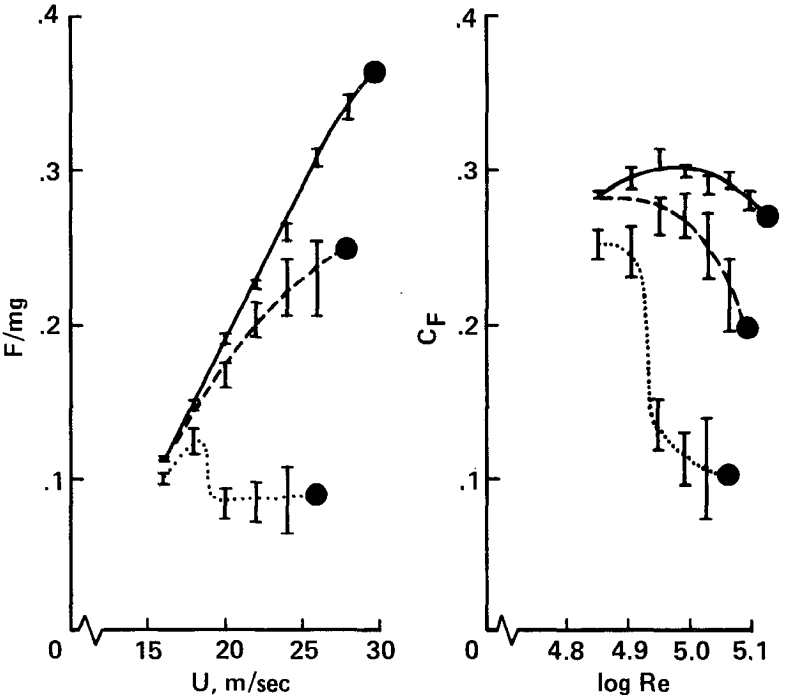

Figure 4 Transverse force on cricket balls as a function of wind speed: ————, new ball; — — — —, 10-over ball; ..... 40-over ball. Bars indicate fluctuations. The seams were fixed at about 30° to the airflow. The transverse forces became intermittent at the points marked ●, and they dropped quickly to zero at higher speeds (Barton 1982).

deliveries), the normalized side force (F/mg, where F is the side force and m is the mass of the ball) is seen to increase with flowspeed up to about 30 m s^{-1}. A nonspinning cricket ball can experience a side force equivalent to almost 40% of its own weight. The side-force coefficient [$C_F = F/(\frac{1}{2}\rho U^2 S)$, where ρ is the air density and S is the ball projected area] also varies with Re and has a maximum value of about 0.3. In a similar setup to Barton's, Hunt (1982) and Ward (1983) made measurements on a large-scale model of a cricket ball. Some typical averaged results for $\alpha = 0°$, but with one side roughened and the other side smooth, are shown in Figure 5. The main advantage here was in being able to investigate the behavior at high Reynolds numbers. The critical value at which C_F starts to decrease is about $\mathrm{Re} = 1.5 \times 10^5$, which corresponds to a flowspeed of about 30 m s^{-1}. The side force starts to decrease when "natural" transition occurs on the nonseam side, which leads to a reduction in the flow asymmetry. It should be noted that fast bowlers in cricket achieve bowling speeds of up to 40 m s^{-1} ($\mathrm{Re} = 1.9 \times 10^5$). The most striking feature in Figure 5 is the appearance of large negative side forces at postcritical Reynolds numbers. Other investigators (Bentley et al. 1982, Horlock 1973) also measured negative side forces at postcritical values of Re. This effect is discussed below in Section 2.4. The variation of C_F with seam angle was also investigated on a smaller model (Figure 6). It is clear that the optimum seam angle is approximately 20° over the whole range of Reynolds numbers investigated. Sherwin & Sproston (1982) mounted a cricket ball on a strain-gauge balance and measured the side force and drag force D on it directly. Figure 7 shows the C_F and C_D [$= D/(\frac{1}{2}\rho U^2 S)$] results for $\alpha = 30°$. The maximum measured value of C_F is about 0.3, which is comparable to Barton's measurements and is also of the same order as the C_D value for the ball (~ 0.45).

2.3 *Spinning Cricket Ball Tests*

When a cricket ball is bowled, with a round arm action as the rules insist, there will always be some backspin imparted to it. The ball is usually held along the seam so that the backspin is also imparted along the seam. At least this is what should be attempted, since a "wobbling" seam will not be very efficient at producing the necessary asymmetric separation.

Barton (1982) and Bentley et al. (1982) measured forces on spinning cricket balls in a wind tunnel by using basically the same technique; the ball was rolled down a ramp along its seam and projected into the airflow. Barton projected the balls through an air jet, whereas Bentley et al. used a closed working section, which made it easier to define boundary conditions for the computation of the forces. The spin rate ω was varied by changing the starting point along the track, and the seam angle was varied by adjusting the alignment of the ramp with the airflow. Once the conditions at

the entry to the wind tunnel and the deflection from the datum are known, the forces due to the airflow can be easily evaluated. Barton calculated the spin rate at the end of the ramp, whereas Bentley et al. measured it by photographing the ball path using a stroboscope. They found that the energy equation used by Barton may have slightly overestimated the spin

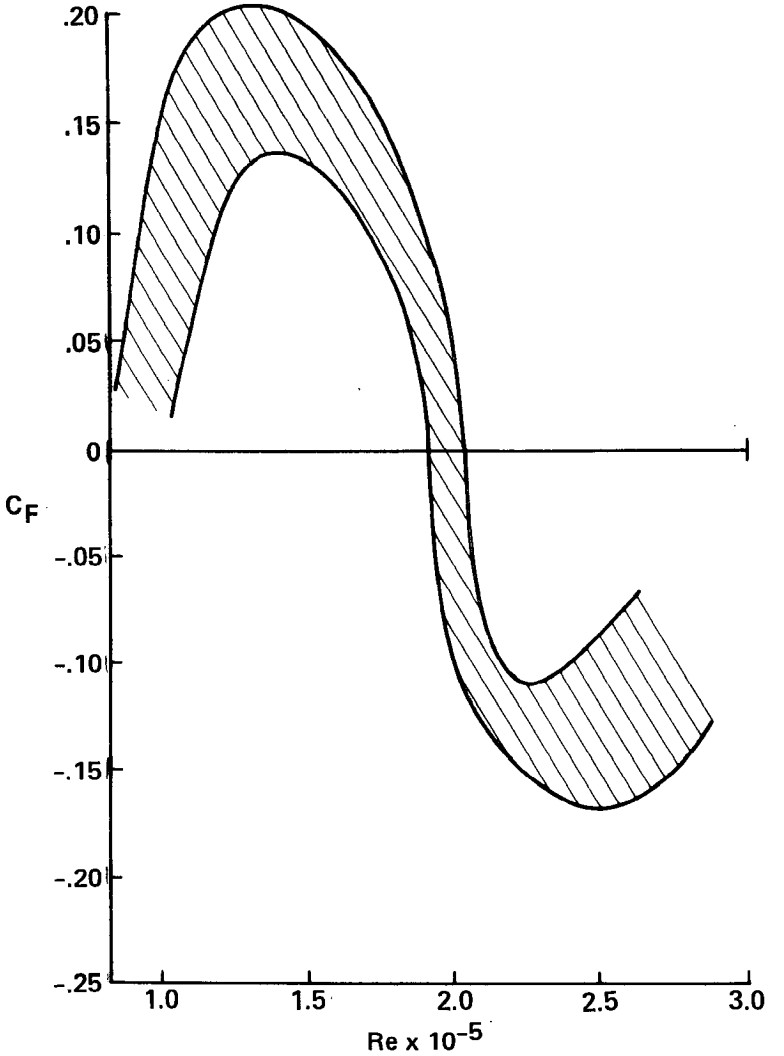

Figure 5 Side-force coefficient measurements on a model cricket ball with one side smooth and the other roughened. Seam angle = 0°; results averaged over eight runs (Hunt 1982).

rate because of the exclusion of the "friction-loss" terms. No account was taken in either investigation of the Magnus force experienced by the spinning balls, although Bentley et al. included a brief discussion on how the measurements may have been affected. The overall accuracy of Bentley et al.'s measurement technique was verified by comparing the C_D results with existing data on spheres.

Barton (1982) found considerable scatter in his measurements, which he

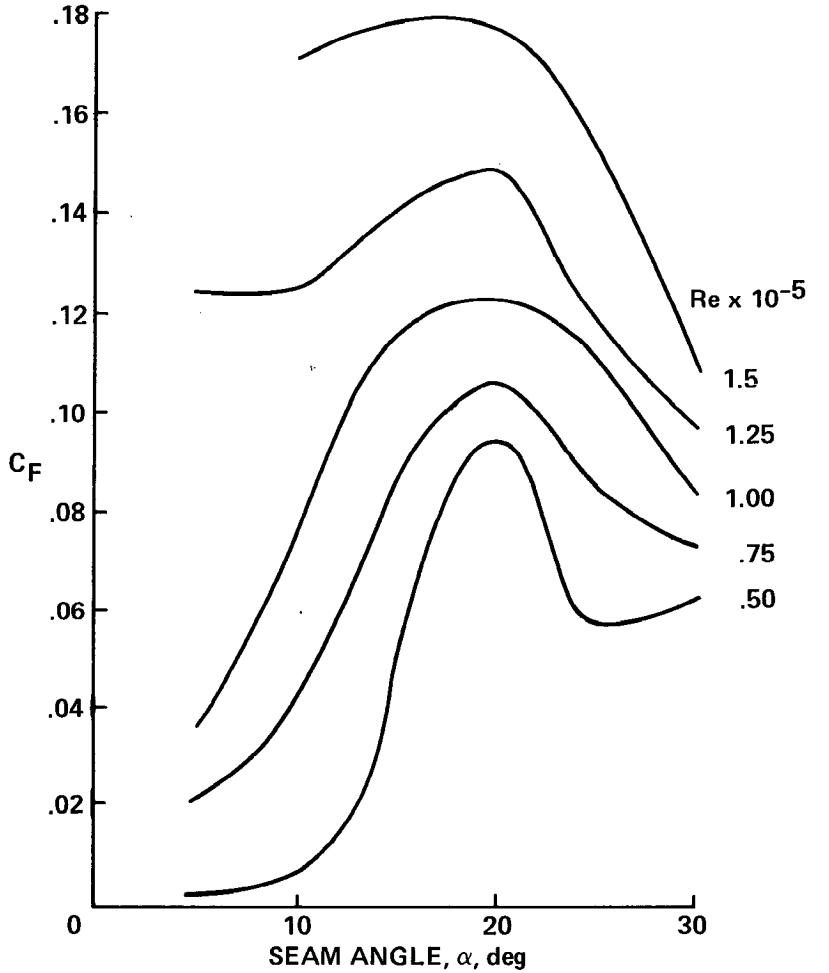

Figure 6 Variation of the side-force coefficient on a model cricket ball with seam angle (Ward 1983).

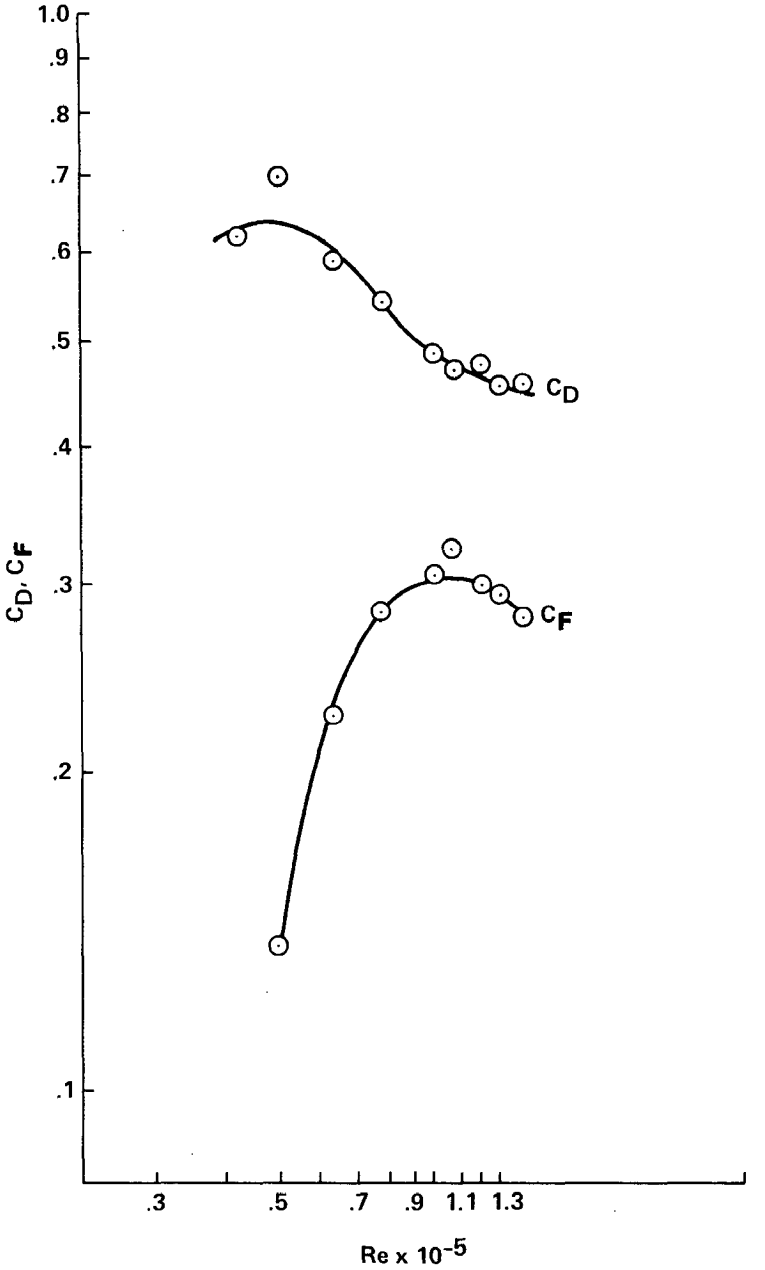

Figure 7 Variation of the side force and drag coefficients on a cricket ball with Reynolds number. Seam angle = 30° (Sherwin & Sproston 1982).

partly attributed to irregular boundary-layer separation. He therefore used a best-fit formula:

$$F/mg = A(U/10)^{\gamma},$$

where the constants A and γ were optimized using a least-squares fit. Barton's best-fit results for each setting are shown in Figure 8. Bentley et al. (1982) also noted considerable scatter, but only in the region of the critical speed ($U \sim 30\,\mathrm{m\,s^{-1}}$) when intermittent transition of the laminar boundary layer on the nonseam side is likely to occur. Figure 9 shows their results, averaged over five balls that were tested extensively. These are averages of

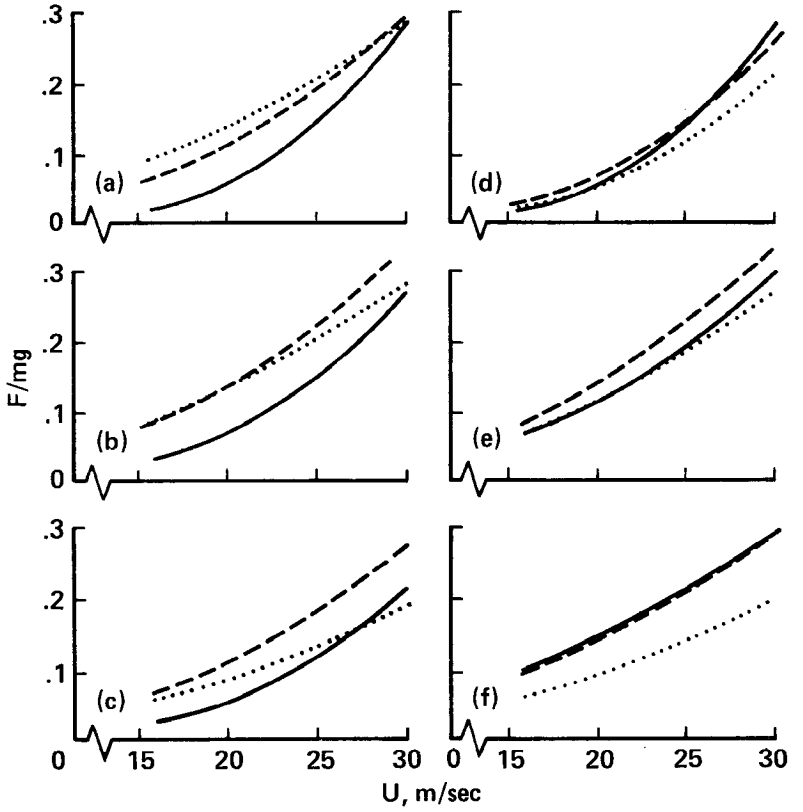

Figure 8 The best-fit approximation to the dimensionless forces, averaged over all cricket balls at the various settings. Left-hand diagrams: (*a*) 2.1 rev s^{-1} spin, (*b*) 4.9 rev s^{-1} spin, (*c*) 9.3 rev s^{-1} spin; ————, 10° seam angle; — — — —, 20° seam angle; ....., 30° seam angle. Right-hand diagrams: (*d*) 10° seam angle, (*e*) 20° seam angle, (*f*) 30° seam angle; ———— 2.1 rev s^{-1} spin; — — — —, 4.9 rev s^{-1} spin; ....., 9.3 rev s^{-1} spin (Barton 1982).

the actual measurements and are not an averaged best-fit. Side forces equivalent to about 30% of the balls's weight are experienced by spinning cricket balls in flight, slightly lower than in the static tests. There is also some dependence of the side force on spin rate. As with the static tests, the critical flowspeed at which the side force starts to decrease in these tests is about 30 m s^{-1}. Therefore, the main results from the two types of testing techniques are comparable.

The actual trajectory of a cricket ball can be computed using the measured forces. Figure 10 shows the computed trajectories at five bowling speeds for the ball exhibiting the best swing properties ($F/mg \sim 0.4$ at $U =$ 32 m s^{-1}, $\alpha = 20°$, $\omega = 14$ rev s^{-1}). The results illustrate that the flight path is almost independent of speed in the range $24 < U < 32$ m s^{-1}. The trajectories were computed using a simple relation, which assumes that the side force is constant and acts perpendicular to the initial trajectory. This gives a lateral deflection that is proportional to time squared and hence a parabolic flight path. By using a more accurate step-by-step model, in

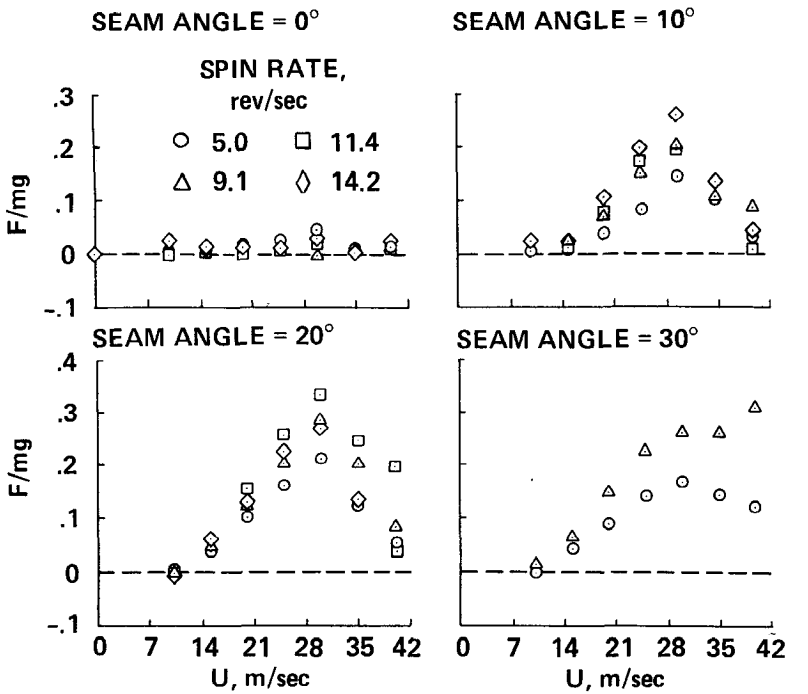

Figure 9 Variation with flowspeed of the normalized side force, averaged over five cricket balls (Mehta et al. 1983).

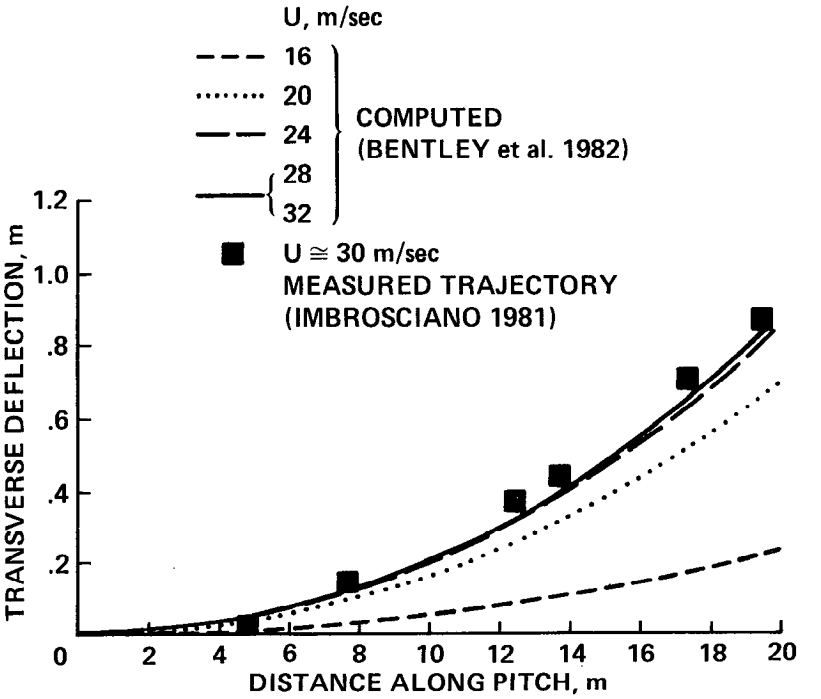

Figure 10 Computed flight paths using measured forces for the cricket ball with the best swing properties. Seam angle = 20°, spin rate = 14 rev s^{-1} (Bentley et al. 1982).

which the side force acted perpendicular to the instantaneous flight direction, R. D. Mehta & T. T. Lim (unpublished results) found that the final deflection was only reduced by about 6%. This calculation also included a semiempirical relation that modeled the change in α due to the movement of the stagnation point as the ball follows a curved flight path. In some photographic studies of a swing bowler, it was confirmed that the trajectories were indeed parabolic (Imbrosciano 1981). These studies also showed that the final predicted deflections of over 0.8 m were not unreasonable. One of the photographed sequences was later analyzed (R. D. Mehta & T. T. Lim, unpublished results), and the actual flight path for this sequence is also plotted in Figure 10. The agreement is excellent considering the crudity of the experimental and analytical techniques.

2.4 *Optimum Conditions for Swing*

It is often suggested that the actual construction of a cricket ball is important in determining the amount of swing obtained. Since some balls

are stitched by hand, these differences can be significant. A two-piece ball is in general found to have better swing properties than a four-piece ball, where the secondary seam produces an effective roughness that helps to cause transition of the laminar boundary layer on the nonseam side. Barton (1982) concluded that a ball with a more pronounced primary seam than average (>1 mm) swung more. However, Bentley et al. (1982) investigated the seam structure on a variety of balls, and while small differences in size and shape were noted, these could not be correlated with the amount of swing. They concluded that, on the whole, the seam on all new balls is efficient at tripping the boundary layer in the speed range $15 < U < 30$ m s^{-1}. It was also apparent that for good swing properties it is perhaps more important to have a perfectly smooth surface on the nonseam side. Both these investigations confirmed that the swing properties of a ball deteriorate with age as the seam is worn and the surface scarred. (In cricket a ball is only replaced by a new one after about 450 deliveries.) There are two other parameters that the bowler can control to some extent: the ball seam angle and the spin rate.

The optimum seam angle for $U \sim 30$ m s^{-1} is found to be about 20° (Figures 6, 8, and 9). At lower speeds (especially for $U < 15$ m s^{-1}) a bowler should select a larger seam angle ($\alpha \sim 30°$), so that by the time the flow accelerates around to the seam, the critical speed has been reached. It is better not to trip the boundary layer too early (low α), since a turbulent boundary layer grows at a faster rate and will therefore separate relatively early (compared with a later tripping). At the same time, the seam angle should not be so large that the boundary layer separates before reaching the seam, since this would result in symmetrical separation on the ball and hence zero side force. In a case like this, if transition occurs in the boundary layer upstream of the seam, then the effect of the seam will be to act as a boundary-layer "fence" that thickens the boundary layer even further. This asymmetry would lead to a negative side force such as that shown in Figure 5 for postcritical Reynolds numbers. This effect can be produced even at low seam angles by inducing early transition of the laminar boundary layer through an increase in the free-stream turbulence. This was confirmed in some experiments performed by Bentley et al. (1982), where significant negative side forces ($F/mg \sim -0.15$) were measured when free-stream turbulence of the same scale as the ball radius was introduced in the wind tunnel.

Spin on the ball helps to stabilize the seam orientation. Basically, for stability, the angular momentum associated with the spin should be greater than that caused by the torque about the vertical axis due to the flow asymmetry. The combination of these two moments can lead to what is commonly known as gyroscopic precession—a moment about the third (horizontal) axis in the plane of the seam that attempts to tumble the ball

over. Although this effect was sometimes observed (Barton 1982, Bentley et al. 1982), it proved rather difficult to correlate with seam angle or spin rate. Too much spin is of course also detrimental, since the effective roughness on the ball's surface is increased (i.e. the critical Reynolds number is reached sooner). This would obviously be more relevant at the higher speeds ($U \sim 25$ m s^{-1}). Barton's (1982) results (Figure 8) seem to indicate that the optimum spin rate is about 5 rev s^{-1}, whereas Bentley et al.'s (1982) results (Figure 9) suggest a much higher optimum spin rate of about 11 rev s^{-1}. The maximum spin rate investigated by Barton was 9.3 rev s^{-1}. While some of this discrepancy may be due to the relatively high turbulence level ($\sim 1\%$) in Barton's wind tunnel (compared with 0.2% in Bentley et al.'s tunnel), the level of the discrepancy is still somewhat surprising. In practice, a bowler can impart spin of up to 14 rev s^{-1}, but it should be noted that this is not an easy parameter to control.

2.5 *Effect of Meteorological Conditions*

The effect of weather conditions is by far the most discussed and controversial topic in cricket. It is widely believed that humid or damp days are conductive to swing bowling, but there has been no scientific proof of this.

The flow pattern around a cricket ball depends only on the properties of the air and the ball itself. The only properties of air that may conceivably be influenced by a change of meteorological conditions are the viscosity or density. Such changes would then affect the ball Reynolds number. However, Bentley et al. (1982) showed that the average changes in temperature and pressure encountered in a whole day would not change the air density and viscosity, and hence the ball Reynolds number, by more than about 2%.

Several investigators (Barton 1982, Horlock 1973, Sherwin & Sproston 1982) have confirmed that no change was observed in the measured pressures or forces when the relative humidity changed by up to 40%.

It has been suggested (Sherwin & Sproston 1982) that humid days are perhaps associated with general calmness in the air and thus less atmospheric turbulence. However, there is no real evidence for this, and even if it were the case, the turbulence scales would be too large to have any significant effect on the flow regime over the ball. Binnie (1976) suggested that the observed increase in swing under conditions of high humidity is caused by "condensation shock" near the point of minimum pressure. This shock would then assist the seam in tripping the laminar boundary layer. However, his calculations showed that this effect could only occur when the relative humidity was nearly 100%. Also, as discussed previously, the seam (on new balls at least) is adequate in tripping the boundary layer in the Reynolds-number range of interest.

The only investigation where the effect of humidity on swing was studied directly is that due to Bentley et al. (1982). They measured surface contours and side forces both on balls that were exposed to high levels of humidity and on balls that were wet completely. As shown in Figures 11*a* and *b*, no significant effect was noted. Photographic tests also showed no discernible effect on the seam or ball surface. Bentley et al. hypothesized that the spin rate imparted to a cricket ball may be affected by damp conditions, since the surface on a new ball becomes tacky and thus allows the bowler a better grip. However, there is no real evidence for this, and so this aspect of cricket ball aerodynamics still remains a mystery.

3. BASEBALL AERODYNAMICS

3.1 *Basic Principles*

Although a baseball has virtually the same size and weight as a cricket ball, there are major differences in the cover design that affect the aerodynamics. The cover of a baseball consists of two hourglass-shaped segments of white leather seamed together by a single row of about 216 stitches (Figure 1). Two basic aerodynamic principles are used to make a baseball curve in flight: spin, and asymmetric boundary-layer tripping due to seam position.

First, consider a curveball. The ball is released so that it acquires top spin about the horizontal axis. The spin produces the Magnus force that makes it curve downward, faster than it would under the action of gravity alone. In this case, the seam produces an overall roughness that helps to reduce the

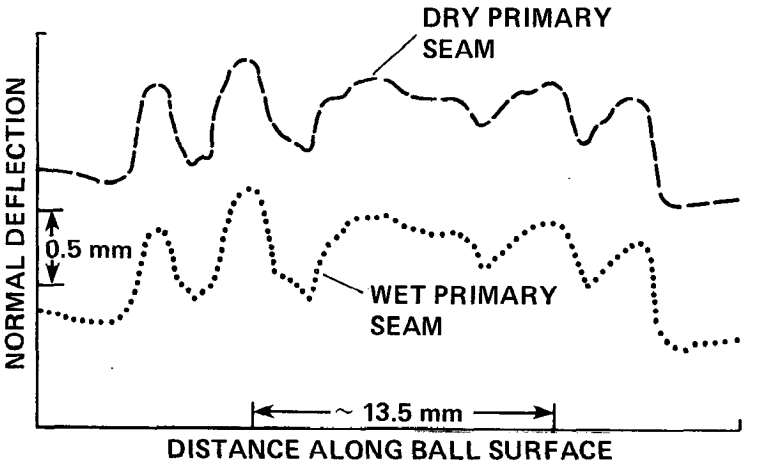

Figure 11a Talysurf contour plots of the primary seam on a cricket ball to investigate effects of humidity (Mehta et al. 1983).

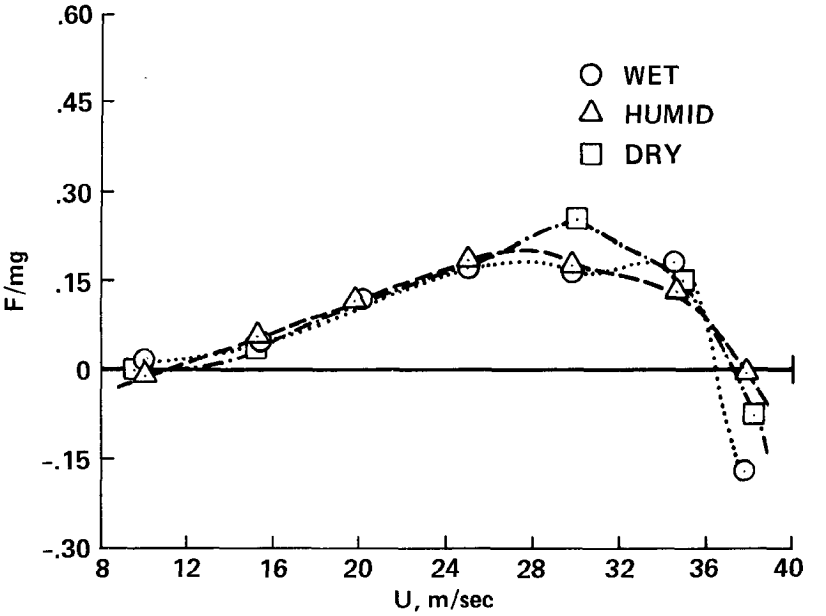

Figure 11b Effect of humidity on the measured side forces on a spinning cricket ball. Seam angle = 20°, spin rate = 5 rev s^{-1} (Bentley et al. 1982).

critical Reynolds number. The pitcher, by varying the angles of his arm and wrist, generates spin about different axes, which produces different rates and directions of curvature. Spin rates of up to 30 rev s^{-1} and speeds of up to 45 m s^{-1} are achieved by pitchers in baseball.

Figure 12 shows a flow-visualization photograph (using smoke) of a baseball held stationary, but spinning counterclockwise at 15 rev s^{-1}, in a wind tunnel with $U = 21$ m s^{-1}. The "crowding together" of smoke filaments over the bottom of the ball shows an increased velocity in this region and a corresponding decrease in pressure. This would tend to deflect the ball downward. Note also the upward deflection of the wake. Thus, a postcritical flow is obtained at these operating conditions.

Second, consider an ideal knuckleball. The ball is released so that it has no spin at all. Then, depending on the position of the seam, asymmetric boundary-layer separation and hence swing can be obtained, much in the same way as with a cricket ball. Although banned over 60 years ago, spit or its modern counterpart, Vaseline, is still sometimes used so that the ball may be squirted out of the fingers at high speed. In Figure 13, the ball is not spinning, but it is so oriented that the two seams trip the boundary layer on the upper side of the ball. The boundary layer on the lower surface is seen to

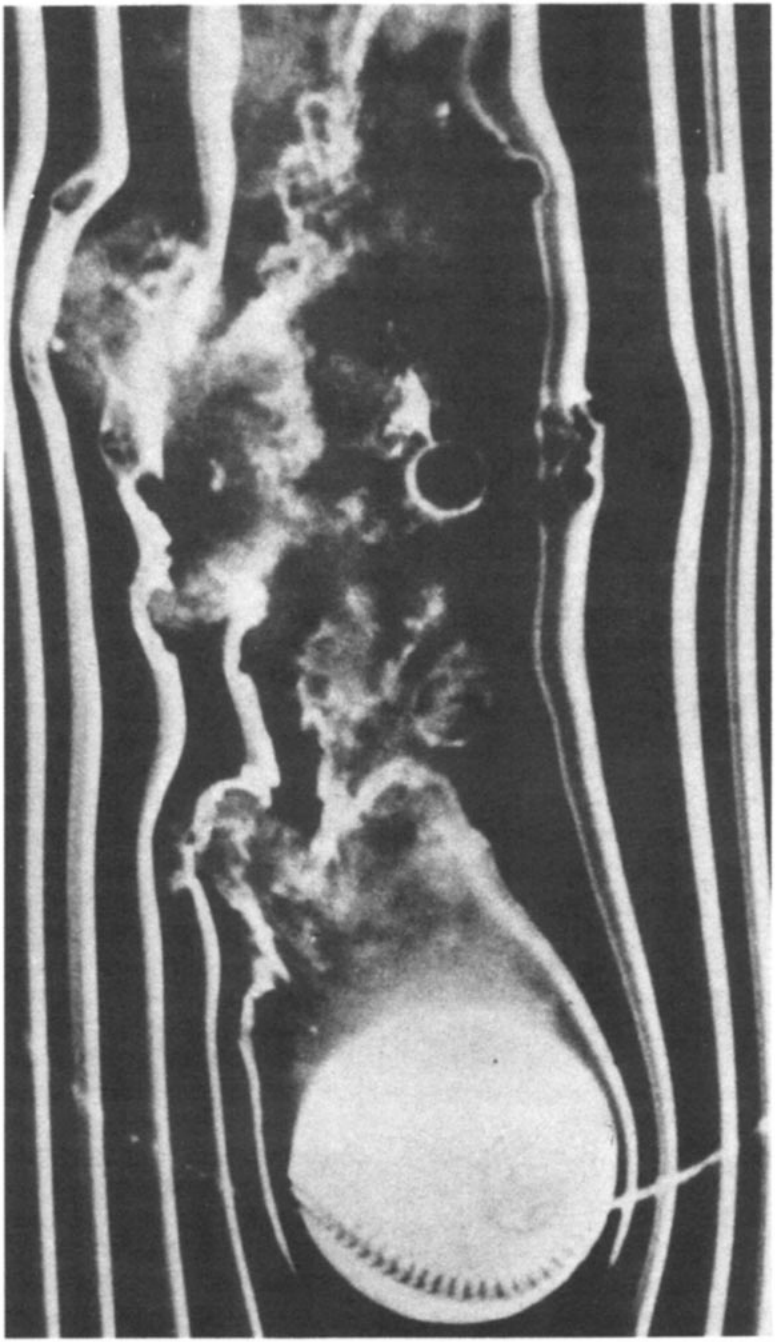

Figure 12 Smoke photograph of flow over a spinning baseball. Flow is from left to right, and the flowspeed is 21 m s^{-1}. The baseball is spinning in a counterclockwise direction at 15 rev s^{-1}. Photograph by F. N. M. Brown, Notre Dame University (Brown 1971).

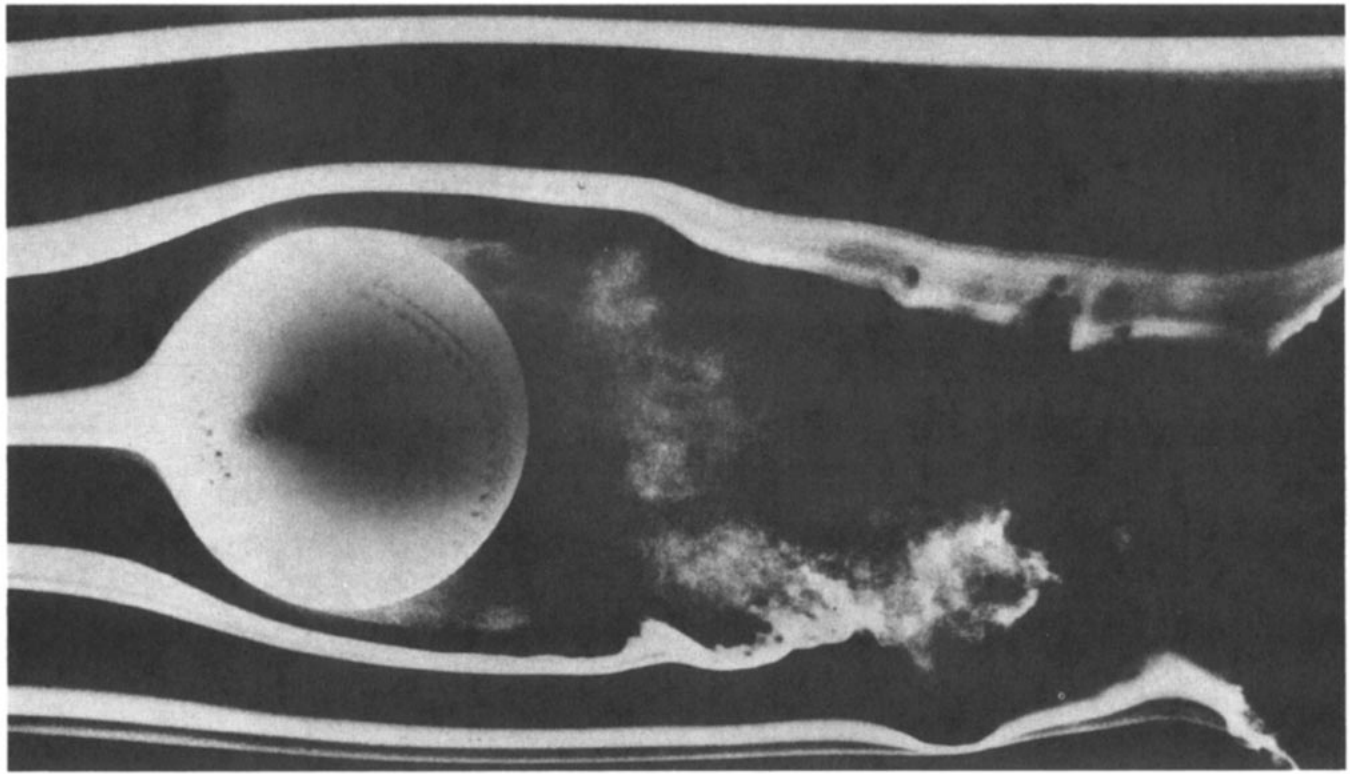

Figure 13 Smoke photograph of flow over a stationary (nonspinning) baseball. Flow is from left to right. Photograph by F. N. M. Brown, Notre Dame University (Brown 1971).

separate relatively early in a laminar state. Once again, the downward deflection of the wake confirms the presence of the asymmetric boundary-layer separation, which would deflect the ball upward.

3.2 *Spinning Baseball Tests (Curveball)*

The effects of spin and speed on the lateral deflection of a baseball were investigated in detail by Briggs (1959). In his first set of experiments, he fired spinning baseballs from an airgun and measured lateral deflections, but this technique did not prove very successful.

In Briggs' (1959) second set of measurements, spinning baseballs were dropped through a 1.8-m wind tunnel. The spinning mechanism was mounted on top of the tunnel and consisted of a suction cup mounted on the shaft that supported the ball. The spinning ball was released by a quick-acting valve that cut off the suction. The lateral deflection was taken as one half of the measured spread of the two points of impact, with the ball spinning first clockwise and then counterclockwise. The spin rate of the spinning mechanism was measured using a stroboscope. The mechanism was aligned so that a baseball spinning about a vertical axis was dropped through a horizontal airstream. Hence, a lateral deflection, perpendicular to the effects due to the drag force and gravity, was produced as a result of the effects of the spin. And since the initial velocity for each run was the same, the deflection gave a direct representation of the lateral force.

In Figure 14, Briggs' measured lateral deflections are illustrated. The straight lines through the origin show that within the limits of experimental accuracy, the lateral deflection is proportional to spin rate. However, Briggs' extrapolation to zero deflection at zero spin is not accurate, since a nonspinning baseball can also develop a lateral force. Hence, the behavior of the lateral force at low spin rates must be nonlinear. In Figure 15, the ratio of deflections is plotted against the ratio of flowspeed, for a given spin rate. Briggs concluded, erroneously, that the implication of the linear relation was that the lateral deflection was proportional to the square of the flowspeed. The graph actually confirms that C_F is independent of Re, which implies that the final deflection is independent of speed. But, once again, this linear relationship is not likely to hold as $U \to 0$ and Reynolds-number effects start to become important. So to summarize Briggs' (1959) results, the lateral deflection of a baseball is directly proportional to spin rate and is independent of the speed for $20 < U < 40$ m s^{-1} and $20 < \omega < 30$ rev s^{-1}.

Briggs (1959) also evaluated the final deflections that would be obtained in practice over the distance of 18.3 m (60 ft). He used a simple model, which assumed that the side force was constant and the distance traveled proportional to the square of the elapsed time, thus giving a parabolic flight path, as for the cricket ball. For $U = 23$ m s^{-1} at $\omega = 20$ rev s^{-1}, a lateral

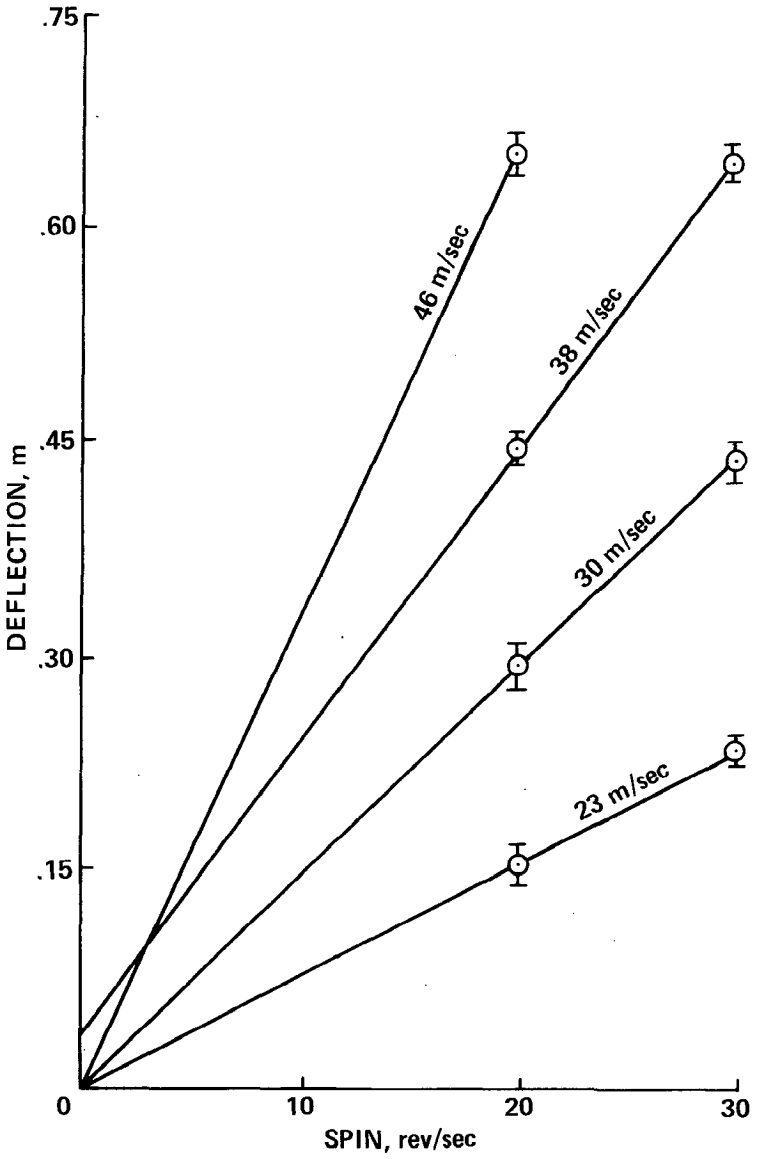

Figure 14 Lateral deflection of a baseball, spinning about a vertical axis, when dropped across a horizontal windstream. These values are all for the same time interval, 0.6 s, the time required for the ball to cross the stream (Briggs 1959).

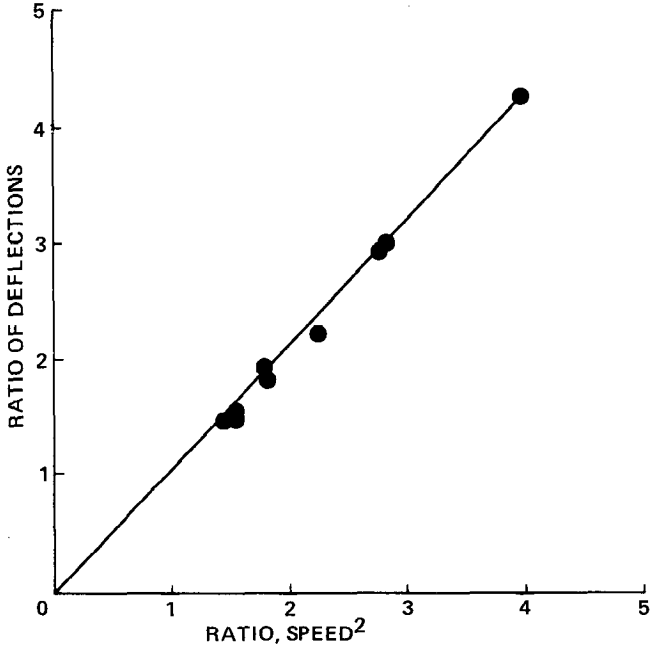

Figure 15 Graph showing that the lateral deflection of a spinning baseball is independent of the flowspeed (Briggs 1959).

deflection of about 0.28 m was obtained, whereas at $\omega = 30$ rev s^{-1}, it was about 0.43 m (corresponding to $F/mg \sim 0.2$). In the case of a curveball, the gravitational force would add to the force due to spin, and so the final deflection would be much greater.

In experiments described by Allman (1982), the actual flight paths of curveballs pitched by a professional were photographed using the stroboscopic technique. Analysis of the flight paths confirmed that the ball travels in a smooth parabolic arc from the pitcher's hand to the catcher, and deflections of over a meter were observed. Therefore, the assumption of a constant side force for a spinning baseball seems to be valid. Since most of the deflection takes place in the second half of the flight, a batter often gets the impression that the ball "breaks" suddenly as it approaches home plate (a slider). However, changes in magnitude and direction of the side force on a ball in flight are not unknown in baseball. This effect is now discussed with reference to knuckleballs.

3.3 *Nonspinning Baseball Tests (Knuckleball)*

Watts & Sawyer (1975) investigated the nature of the forces causing the "erratic motions" of a knuckleball. The lateral force on a baseball held

stationary in a wind tunnel was measured and correlated with seam orientation. The lateral force and drag were measured by mounting a baseball on a calibrated strain-gauge balance.

The datum position of the baseball is defined in Figure 16*a*, and Figure 16*b* shows the measured forces on the ball at $U = 21\ \mathrm{m\,s^{-1}}$, for $\phi = 0$–360°. At $\phi = 0°$, the normalized lateral force (F/mg) was zero, but as the ball orientation was changed, values of $F/mg = \pm 0.3$ were obtained with large fluctuations ($F/mg \sim 0.6$) at $\phi = 50°$. These large fluctuating forces were found to occur when the seam of the baseball coincided approximately with the point where boundary-layer separation occurs, an angle to the vertical of about 110°. The separation point was then observed to jump from the front to the back of the stitches and vice versa, thereby producing an unsteady flow field. The frequency of the fluctuation was of the order of 1 Hz, a value low enough to cause a change of direction in the ball's flight. A discontinuous change in the lateral force was also observed at $\phi = 140$ and 220°. Watts & Sawyer (1975) concluded that this was associated with the permanent movement of the separation point from the front to the rear of the seam (or vice versa). They claim that the data near all four of the "critical" positions ($\phi = 52$, 140, 220, and 310°) were "quite repeatable."

Figure 17 shows the variation of the difference between maximum and minimum lateral forces with flowspeed, while Figure 18 shows the variation

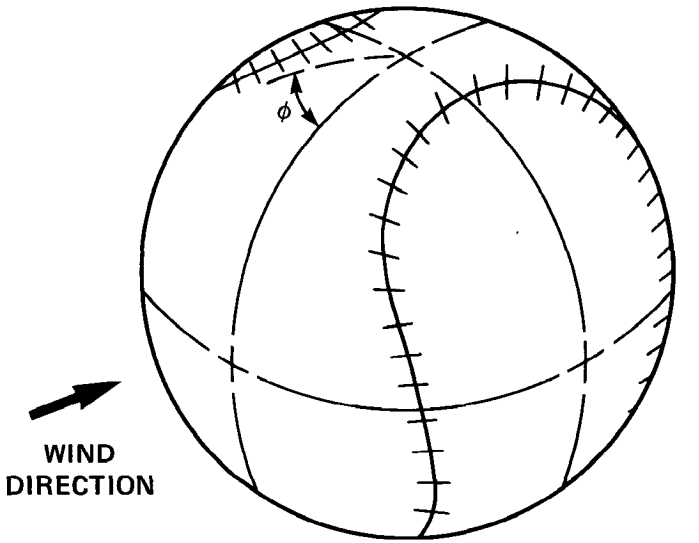

Figure 16a Datum position of baseball at $\phi = 0°$. The ball can be rotated in the direction ϕ to a new position (Watts & Sawyer 1975).

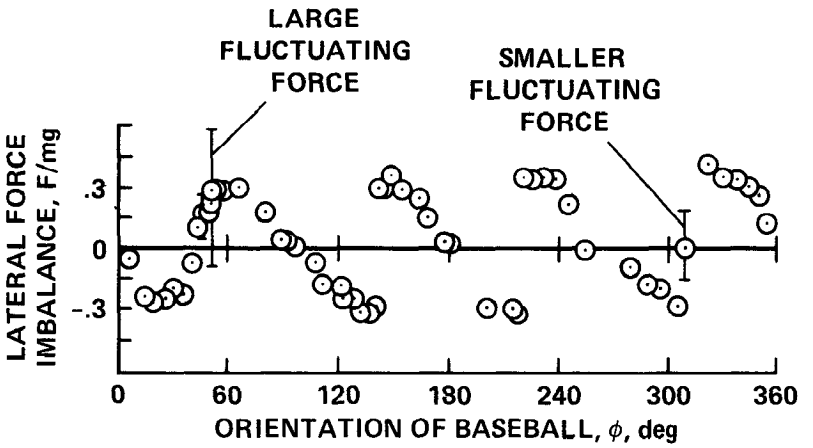

Figure 16b The variation of the lateral force imbalance with orientation of the baseball—see Figure 16*a* for definition of ϕ (Watts & Sawyer 1975).

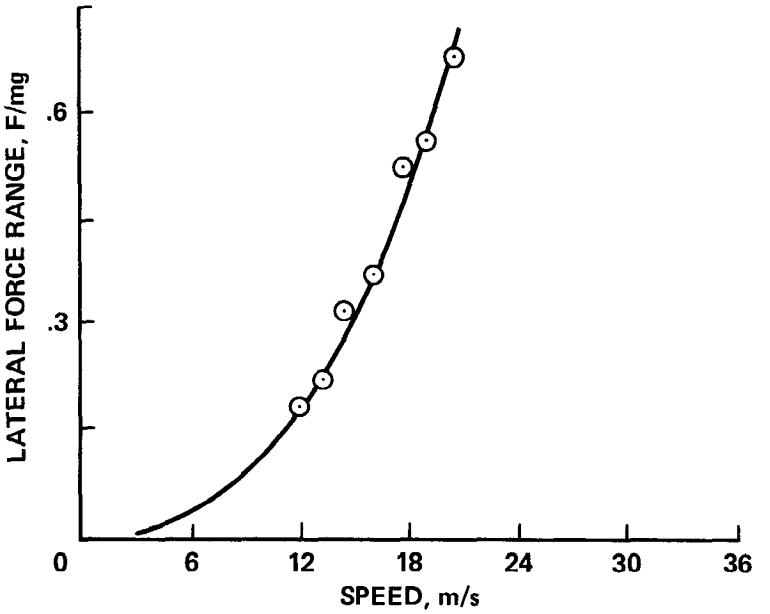

Figure 17 Variation of difference between the maximum and minimum lateral forces on a baseball (Watts & Sawyer 1975).

of the fluctuating force near $\phi = 52$ and 310°. Since the magnitudes of the forces increase approximately as U^2, the lateral deflection for the knuckleball would also be independent of flowspeed within the range considered ($12 < U < 20$ m s^{-1}). The fluctuating force frequency was also found to be almost independent of flowspeed.

Watts & Sawyer (1975) computed some trajectories using their measured forces and the same simple assumption as Bentley et al. (1982) and Briggs (1959)—namely, that the lateral force on the baseball acts in a direction perpendicular to the original direction of level flight. The lateral force was assumed to be periodic in time, which implied that the lateral deflection would decrease with increasing spin. Some computed trajectories for the cases when the ball was initially oriented at $\phi = 90°$ and spin imparted such that the ball rotated a quarter- or a half-revolution during its flight to the home plate are illustrated in Figure 19. Clearly, the pitch with the lower spin rate has the maximum deflection and change of direction and would therefore be the more difficult one to hit. For the erratic flight of a knuckleball, Watts & Sawyer (1975) suggest that this could happen when

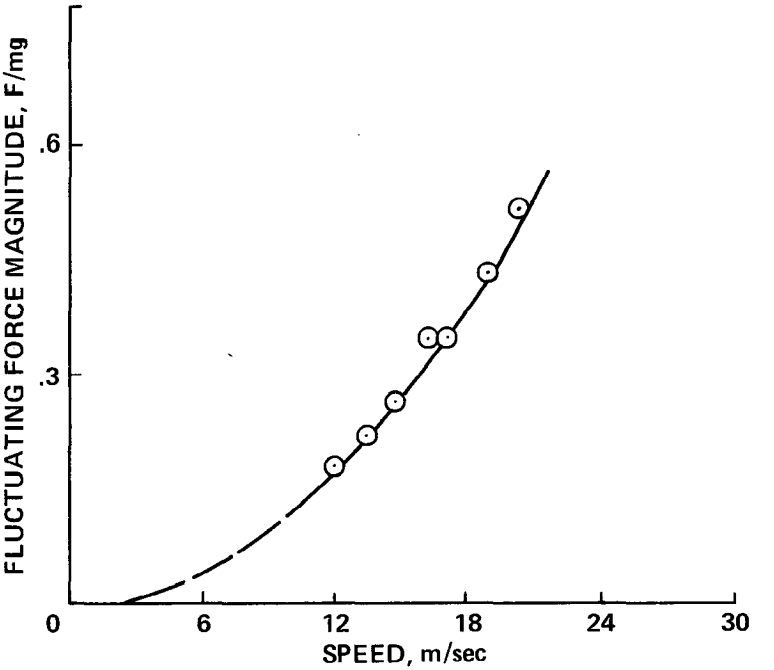

Figure 18 Variation of the magnitude of the fluctuating force on a baseball (Watts & Sawyer 1975).

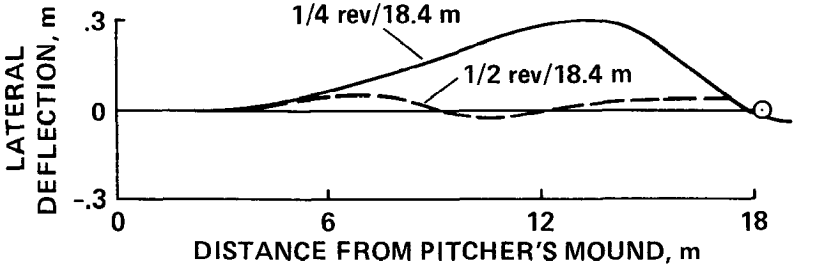

Figure 19 Typical computed trajectories for a slowly spinning baseball, with $U = 21$ m s^{-1} (Watts & Sawyer 1975).

the ball is so released that the seam lies close to the separation point. However, as Weaver (1976) rightly points out, a baseball thrown with zero or near-zero spin will experience a torque due to the flow asymmetry that will cause the ball to rotate. This is similar to the stability problem discussed in Section 2.4 for the cricket ball. It therefore seems that in practice it would be difficult to pitch a baseball that maintains, for the whole flight, an attitude where the erratic lateral force occurs. Thus, sudden changes in flight path are probably not as common as baseball players claim. And indeed, on studying the actual flight paths of professionally pitched knuckleballs (Allman 1983), it was found that while the direction of lateral deflection was unpredictable, there were no sudden, erratic changes in flight path.

4. GOLF BALL AERODYNAMICS

4.1 *Basic Principles*

Golfing legend has it that in about the mid-nineteenth century a professor at Saint Andrews University discovered that a gutta-percha ball flew farther when its surface was scored (Chase 1981). This discovery soon became common knowledge, and it sparked off numerous cover designs, chosen more or less by intuition. Balls with raised patterns were not very successful, since they tended to collect mud and presumably also experienced a larger drag force. Covers with square and rectangular depressions were also tried, but by about 1930, the ball with round dimples had become accepted as the standard design. A conventional golf ball has either 330 (British ball) or 336 (American ball) round dimples arranged in regular rows (Figure 1).

In golf ball aerodynamics, apart from the lift force (which is generated by the backspin imparted to the ball), the drag and gravitational forces are also important, since the main objective is to obtain maximum distance in flight.

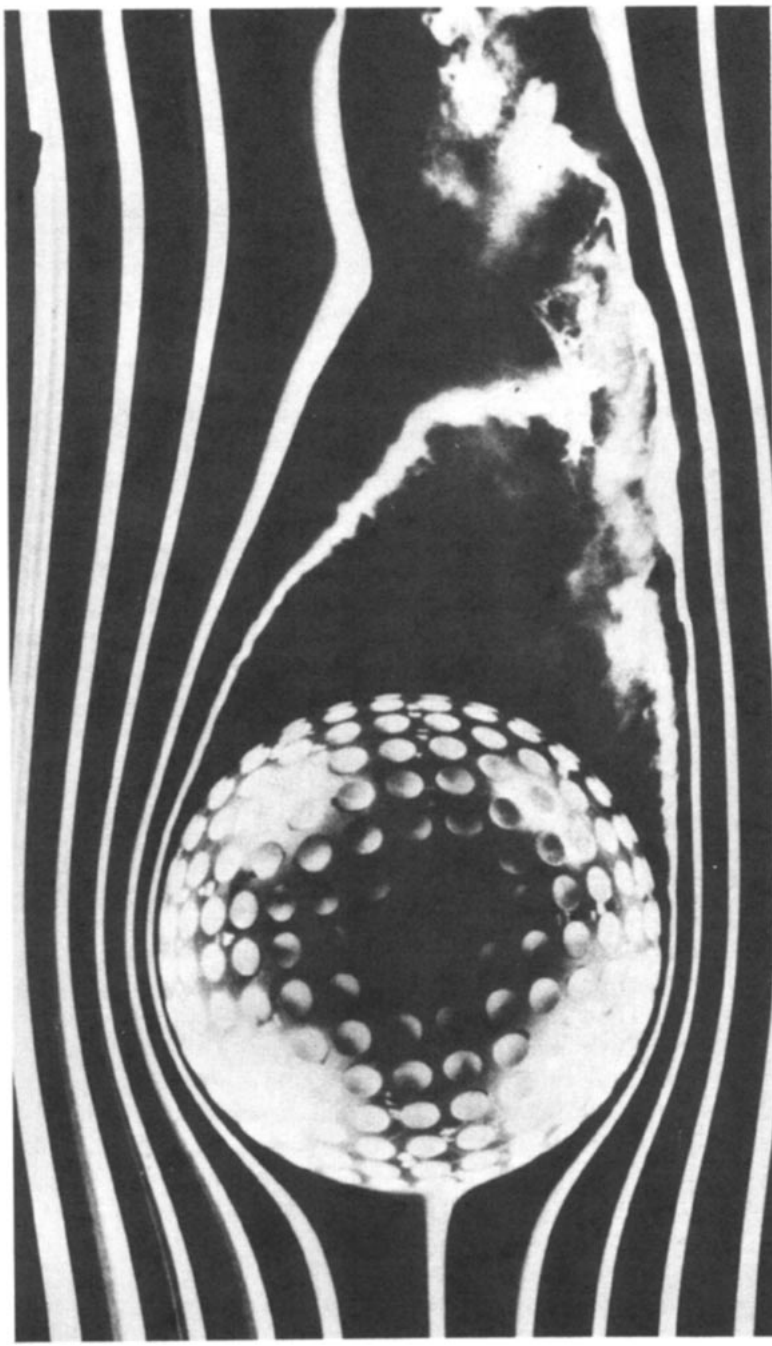

Figure 20 Smoke photograph of flow over a clockwise-spinning golf ball. Flow is from left to right. Photograph by F. N. M. Brown, Notre Dame University (Brown 1971).

At postcritical Reynolds numbers, the effect of spin is to delay separation on the upper (retreating) side and to advance it on the lower (advancing) side. In the smoke photograph of a clockwise spinning golf ball (Figure 20), the asymmetric separation and the downward-deflected wake are clearly illustrated, thus indicating a normal (upward) force on the ball. The effect of the dimples is to lower the critical Reynolds number. Figure 21 illustrates how dimples are more effective than, for example, sand-grain roughness at reducing the critical Reynolds number. The rapid rise in C_D for the sphere with sand-grain roughness is due to the forward movement of the transition point and the artificial thickening of the boundary layer by the roughness elements. The golf ball C_D value does not rise in this way, which indicates that dimples are effective at tripping the boundary layer without causing the thickening associated with positive roughness. The lift and drag coefficients are functions of Reynolds number and a spin parameter—the one normally used is V/U, where V is the equatorial speed of the ball. Unlike cricket and baseball, in golf both Re and V/U will change significantly during a typical flight, which means that C_L and C_D must also be expected to vary.

Typically, a golf ball is driven at an initial velocity of 75 m s^{-1} with the ball spinning backward at 3500 rpm, or about 60 rev s^{-1}. (Since the spin rates in golf are relatively high, they are conventionally quoted in rpm.) This gives a spin parameter of about 0.1 and a Reynolds number based on ball diameter (41.1 mm) of about 2.1×10^5.

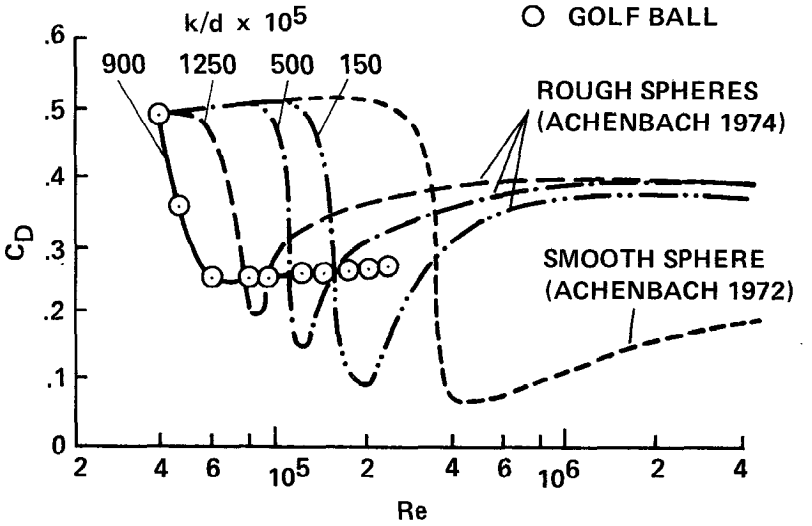

Figure 21 Variation of golf ball and sphere drag, where k is the sand-grain roughness height and d is the ball diameter (Bearman & Harvey 1976).

4.2 *Measurements of Forces on Golf Balls*

Davies (1949) measured the aerodynamic forces on golf balls by dropping spinning balls through a wind-tunnel working section. The ball was held between two shallow cups that were rotated with a variable speed motor (equipped with a tachometer) about a horizontal axis perpendicular to the airstream. A trigger released the springs on the cups, and the ball was allowed to drop through the airstream. The landing spot was marked on waxed paper, and by spinning the ball in one direction and then the other, the drag and lift forces could be evaluated. Davies claimed that the overall error in the measured forces was less than 10%. Spin rates of up to 8000 rpm were investigated at a flowspeed of about 32 m s^{-1}. This gave a Reynolds number based on ball diameter (42.7 mm) of about 9.4×10^4, somewhat lower than that attained by a ball leaving the tee ($\sim 2.1 \times 10^5$).

Bearman & Harvey (1976) measured the aerodynamic forces on model balls over a wide range of Reynolds numbers (0.4×10^5–2.4×10^5) and spin rates (0–6000 rpm). The two and one-half times full-scale models were constructed as hollow shells. A motor and bearing assembly on which the ball revolved was installed within the model. The model was supported from a wire, 0.5 mm in diameter ($\equiv 0.5\%$ of the model diameter). The upper support wire was attached to a strain-gauged arm, which in turn was mounted on a three-component force balance. The spin rate of the ball was measured using a stroboscope. Bearman & Harvey confirmed that the interference due to the support wires was minimal by comparing the C_D measurements on a nonrotating smooth sphere with previous data.

The results from both of these investigations (Davies 1949, Bearman & Harvey 1976) are shown in Figure 22 for a Reynolds number of about 10^5. The variation of C_L and C_D with V/U obtained by Davies has the same overall trends as the data due to Bearman & Harvey. At a spin rate of about 8000 rpm, Davies measured lift forces equivalent to about one half the weight of the ball and drag forces that were equal to the weight of the ball. He proposed a semiempirical relation for the lift force:

$$L = 0.029\,[1 - \exp(-0.00026N)],$$

where N is the spin rate in revolutions per minute and L is the lift in kilograms. However, as Bearman & Harvey (1976) point out, this nonlinear behavior most likely results from Davies' low Reynolds number. The measurements due to Bearman & Harvey are probably more representative and accurate.

Figures 23 and 24 show the variation of C_L and C_D, respectively, with varying spin. On the whole, C_L is found to increase with spin, as one would expect, and C_D also increases as a result of induced drag effects associated

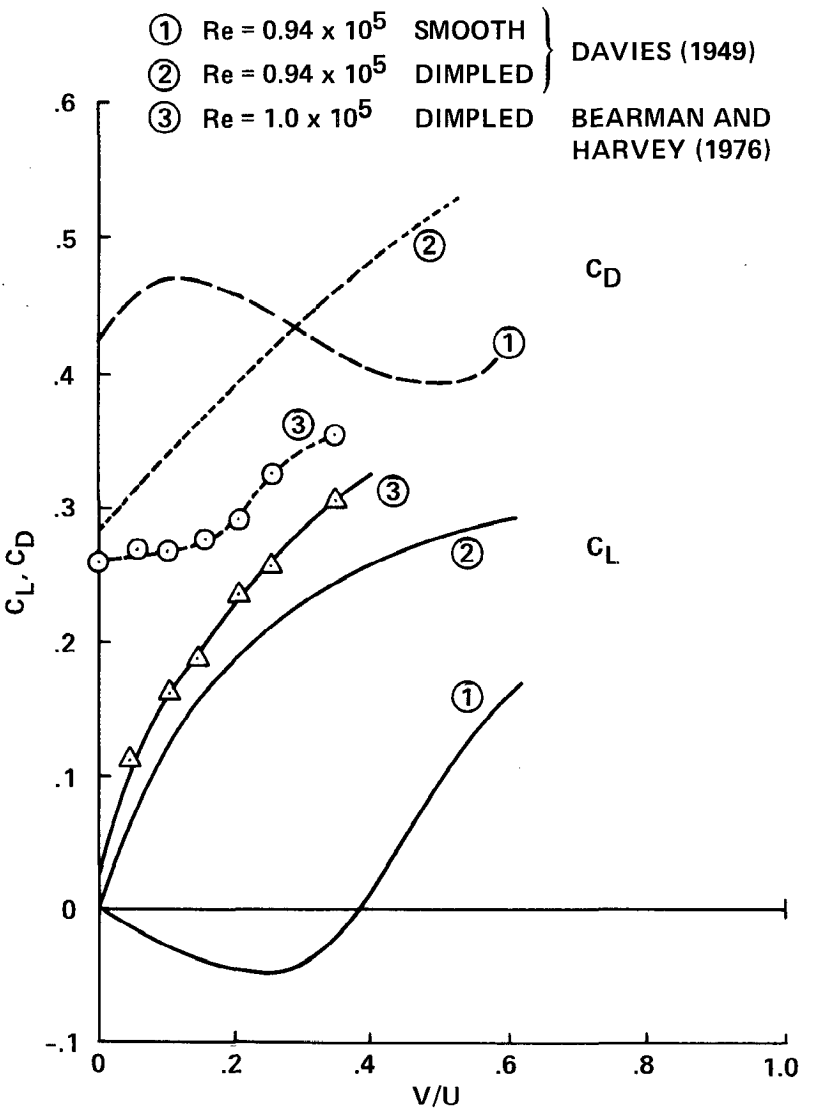

Figure 22 Lift and drag coefficients of rotating spheres and golf balls plotted against spin parameter (Bearman & Harvey 1976).

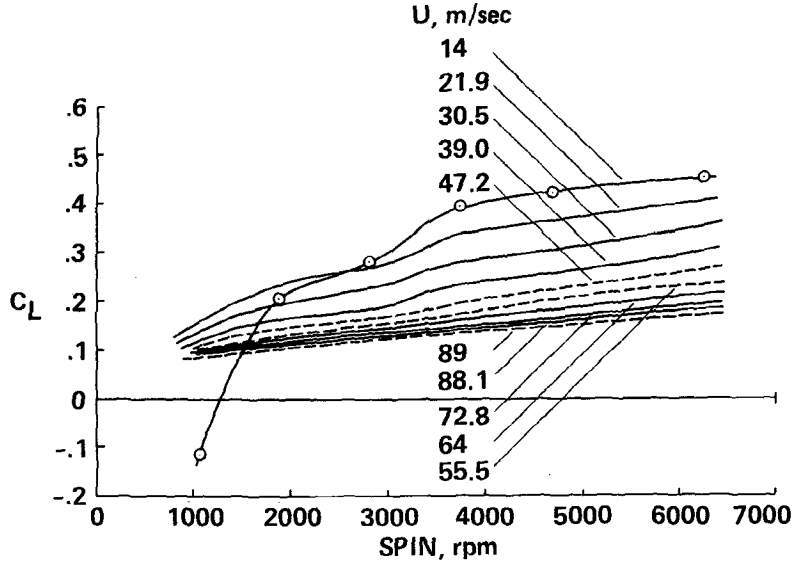

Figure 23 Lift coefficient of a conventional (British) golf ball (Bearman & Harvey 1976).

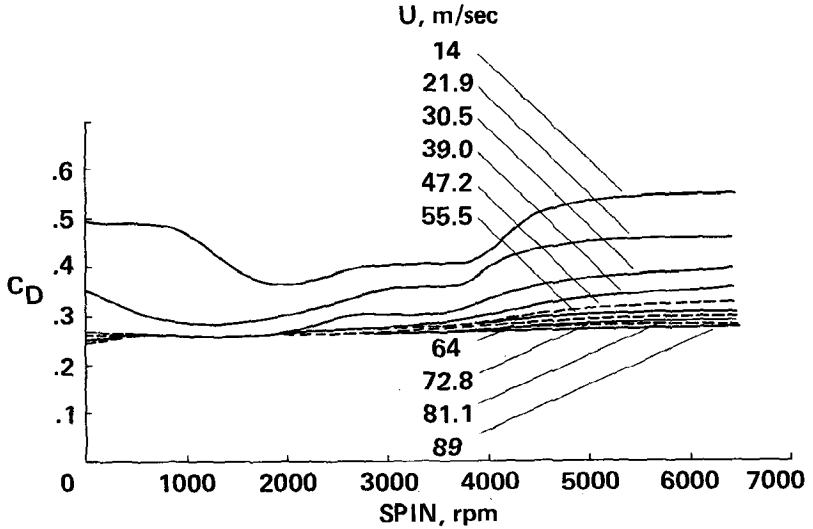

Figure 24 Drag coefficient of a conventional (British) golf ball (Bearman & Harvey 1976).

with lifting bodies. At a given spin rate, increasing U decreases the spin parameter, and hence C_L and C_D are also reduced. At postcritical Reynolds numbers, the relation between lift and spin rate is almost linear, as in the case of a baseball. However, this linear relationship does not hold as $N \to 0$; and for $U \sim 14$ m s^{-1} and $N < 1200$ rpm, a negative lift is obtained at this precritical Reynolds number. Bearman & Harvey (1976) conclude that the lift in this regime "cannot be explained by any simple attached flow circulation theory." This situation mainly results from the fact that transition is a very unstable phenomenon, which is easily influenced by parameters such as the details of the local surface roughness and free-stream turbulence.

4.3 *Computation of Golf Ball Trajectories*

Bearman & Harvey (1976) computed complete golf ball trajectories using the measured aerodynamic forces. The computation involved a step-by-step calculation procedure of the two components of the equation of motion:

$$\ddot{x} = -\frac{\rho S}{2m}(\dot{x}^2+\dot{y}^2)(C_D \cos\beta + C_L \sin\beta),$$

$$\ddot{y} = \frac{\rho S}{2m}(\dot{x}^2+\dot{y}^2)(C_L \cos\beta - C_D \sin\beta) - g,$$

where x and y are measured in the horizontal and vertical directions, respectively, and β is the inclination of the flight path to the horizontal [i.e. $\beta = \tan^{-1}(\dot{y}/\dot{x})$]. At each time step, the measured values (or interpolations) of C_L and C_D were used. The amount of spin decay during flight is difficult to predict. However, Bearman & Harvey tried some realistic assumptions, including the one wherein the decay was assumed to be proportional to N^2, and found that the computed trajectories were not affected significantly.

Figure 25 shows a computed trajectory for initial conditions typical of a professional golfer's drive. Note that toward the end of the flight, as the velocity decreases, the aerodynamic forces lose importance to the gravitational force.

The effect on range of the three main initial parameters (spin rate,

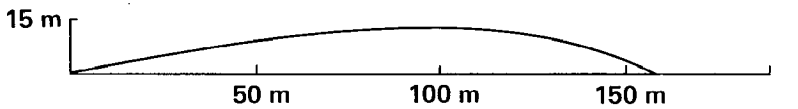

Figure 25 Computed golf ball trajectory. Initial conditions: velocity = 57.9 m s^{-1}, elevation = 10°, spin = 3500 rpm (Bearman & Harvey 1976).

velocity, and elevation) are shown in Figures 26*a*, *b*, and *c*, respectively. In Figure 26*a*, the maximum range for the initial conditions given is obtained for a spin rate just over 4000 rpm. In Figure 26*b*, the range increases rapidly with velocity for initial velocities greater than about 30 m s^{-1}. The range seems to be a relatively weak function of the initial elevation, although it is still increasing at an initial elevation angle of 15°. In practice, as Bearman & Harvey (1976) point out, hitting the ball harder increases both the initial velocity and spin. Bearman & Harvey (1976) also compared the ranges computed from the wind-tunnel results with actual measured values using golf balls launched by a driving machine. In general, the ball traveled slightly farther than predicted. This was attributed to incorrect scaling of the dimple edge radius.

4.4 *Effect of Dimple Geometry*

The results discussed in Section 4.3 clearly show that the aerodynamics of a golf ball depend critically on the flow induced by the dimples. The actual geometry of the dimples must therefore be expected to affect the flow regime

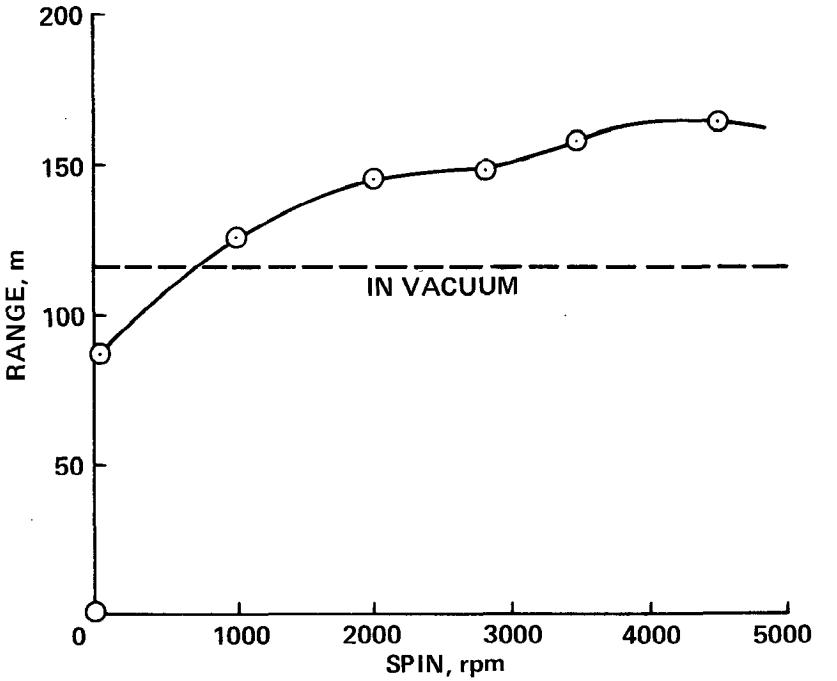

Figure 26a Effect of spin on range for a conventional (British) golf ball. Initial conditions: velocity = 57.9 m s^{-1}, elevation = 10° (Bearman & Harvey 1976).

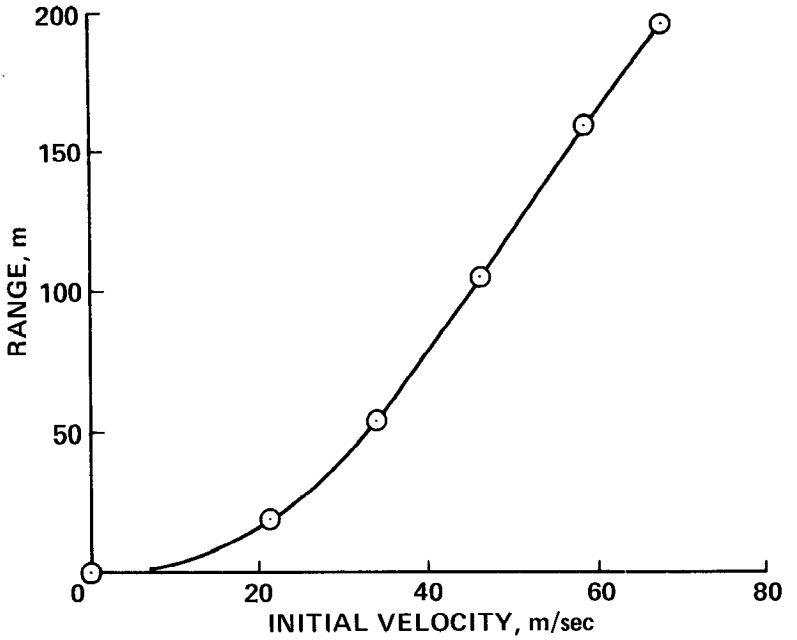

Figure 26b Effect of initial velocity on range for a conventional (British) golf ball. Initial conditions: elevation = 10°, spin = 3500 rpm (Bearman & Harvey 1976).

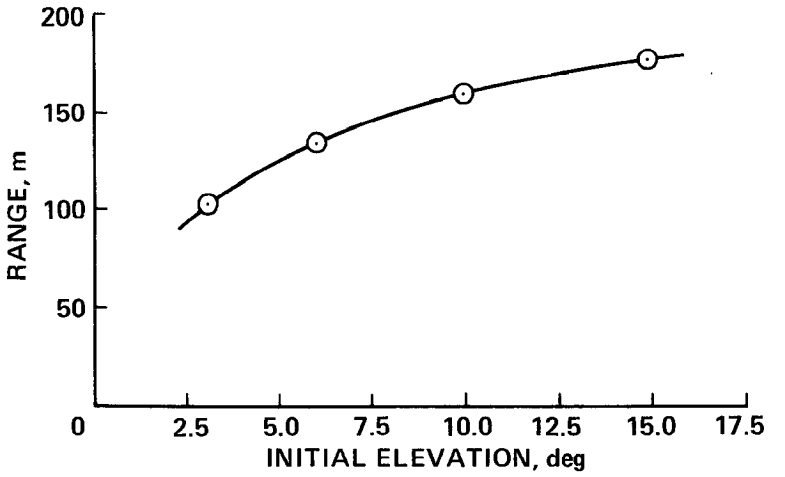

Figure 26c Effect of initial elevation on range for a conventional (British) golf ball. Initial conditions: velocity = 57.9 m s^{-1}, spin = 3500 rpm (Bearman & Harvey 1976).

and hence the aerodynamic forces on the golf ball. While this particular effect is difficult to understand and to quantify accurately, some experiments (described below) have been performed to establish its importance.

In general, for a given geometry and Reynolds number, the dimples would have to be deep enough to cause a disturbance in the laminar boundary layer. However, if the dimples are too deep, this may contribute to the drag force, although the actual mechanism causing it is not obvious. So there must be an optimum depth for the dimples at a given Reynolds number. This is shown to be the case in Figure 27, where the effect of square dimple depth on range is illustrated. The golf ball was launched by a driving machine. Clearly there is an optimum depth of about 0.25 mm at which the range is maximum.

Bearman & Harvey (1976) investigated the effects of changing the dimple shape. Apart from the model ball of conventional design, they also measured forces on a "hex-dimpled" ball, which had 240 hexagonal dimples and 12 pentagonal dimples arranged in a triangular pattern. The results for the postcritical regime are compared in Figure 28. In general, the hex-dimpled ball is superior to the conventional ball: it exhibits higher lift and

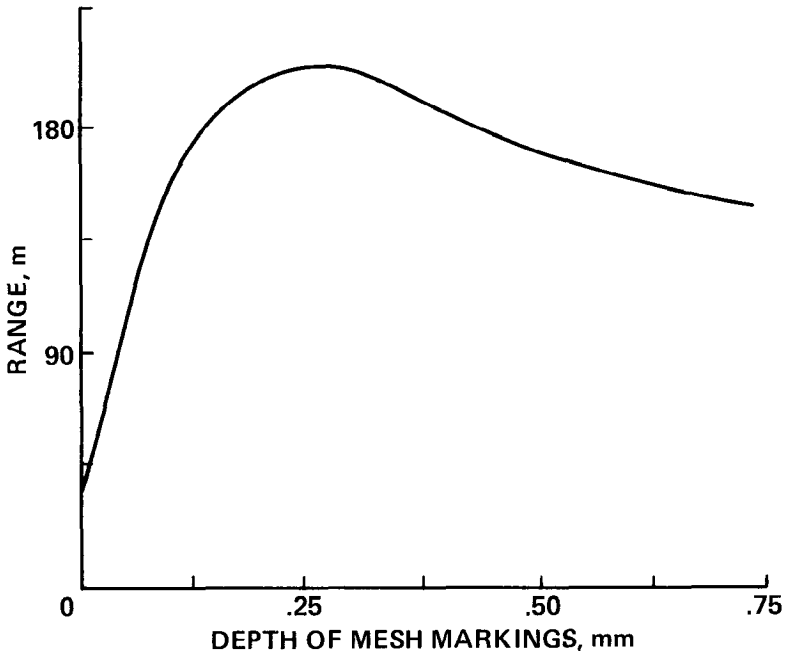

Figure 27 Effect of square dimple depth on range (Cochran & Stobbs 1968).

lower drag properties. Tests using a driving machine showed that under normal driving conditions the hex-dimpled ball traveled approximately 6 m farther than a conventional ball. Bearman & Harvey conclude that "hexagonal shaped dimples act as even more efficient trips than round dimples, perhaps by shedding into the boundary layer more discrete (horse-shoe) vortices from their straight edges."

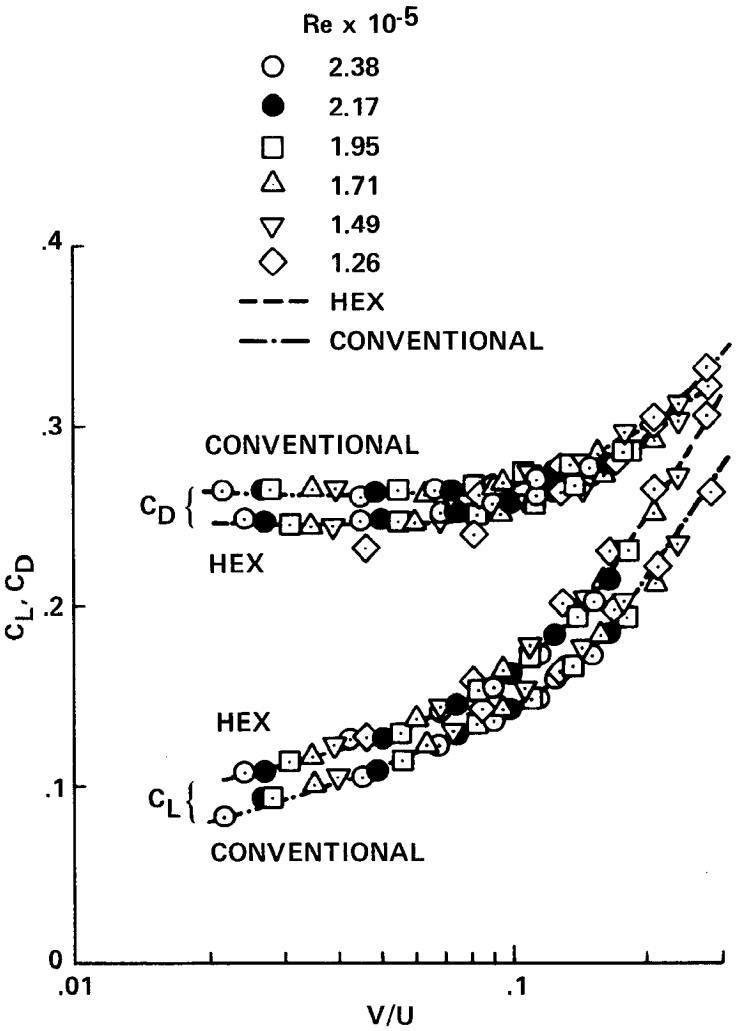

Figure 28 Comparison of conventional and hex-dimpled (British) golf balls (Bearman & Harvey 1976).

Apart from the dimple size and shape, the arrangement of dimples also seems to be a relevant parameter. A conventional golf ball has a "seam" with no dimples along the equator, where the two molded halves join together. At the relatively high Reynolds numbers and spin rates encountered in golf, this seam could produce an asymmetric flow, as on a cricket ball. This is of concern to (professional) golfers, and one of the new designs has 10 seams, which makes the ball more isotropic (Cavendish 1982). On the other hand, a ball was also designed that had dimples only on a band along the seam (Chase 1981). Presumably, the idea behind this design is that when the ball is driven off the tee, with the dimples in the vertical plane, it would generate roughly the same amount of lift as a conventional ball if it spins about the horizontal axis only. However, if the ball is sliced, so that it rotates about a near-vertical axis, the reduced overall roughness would increase the critical Reynolds number, and hence the sideways (undesirable) deflection would be reduced.

5. CONCLUDING REMARKS

Large lateral forces, equivalent to about 50% of the ball's weight, can be generated by sports balls in flight. This corresponds to a side force or lift coefficient of about 0.3. The mechanism responsible is asymmetric boundary-layer separation, achieved either by fence tripping at precritical Reynolds numbers [as on a cricket ball and nonspinning baseball (knuckleball)] or by spin-induced effects, which generate a postcritical, asymmetric flow [as on a baseball (curveball) and golf ball].

The most popular and effective method for measuring aerodynamic forces on balls is to release them (spinning) through an airstream and measure the deflection due to the side force. This technique is only useful when the side force is constant during flight. The assumption of constant side force seems to be valid for spinning baseballs and cricket balls; it results in a deflection that is proportional to the square of elapsed time, and hence in a parabolic flight path. More sophisticated models are necessary for a nonspinning baseball and for a golf ball, since the forces on these balls change magnitude and direction during flight. However, abrupt changes in force magnitude or direction, resulting in abrupt changes in flight path, are probably not very common in practice.

ACKNOWLEDGMENTS

I am grateful to Tee Lim for help with the cricket ball trajectory computations and to Jim Walton for helpful discussions on baseball

aerodynamics. I would also like to thank all my colleagues at the Ames Research Center who reviewed an earlier draft of this article.

This article is dedicated to my late father.

Literature Cited

Achenbach, E. 1972. Experiments on the flow past spheres at very high Reynolds numbers. *J. Fluid Mech.* 54:565–75

Achenbach, E. 1974. The effects of surface roughness and tunnel blockage on the flow past spheres. *J. Fluid Mech.* 65:113–25

Allman, W. F. 1982. Pitching rainbows. *Sci. 82* 3(8):32–39

Allman, W. F. 1983. Flight of the knuckler. *Sci. 83* 4(5):92–93

Barkla, H. M., Auchterlonie, L. J. 1971. The Magnus or Robins effect on rotating spheres. *J. Fluid Mech.* 47:437–47

Barton, N. G. 1982. On the swing of a cricket ball in flight. *Proc. R. Soc. London Ser. A* 379:109–31

Bearman, P. W., Harvey, J. K. 1976. Golf ball aerodynamics. *Aeronaut. Q.* 27:112–22

Bentley, K., Varty, P., Proudlove, M., Mehta, R. D. 1982. An experimental study of cricket ball swing. *Aero Tech. Note 82–106*, Imperial Coll., London, Engl.

Binnie, A. M. 1976. The effect of humidity on the swing of cricket balls. *Int. J. Mech. Sci.* 18:497–99

Brancazio, P. J. 1983. The hardest blow of all. *New Sci.* 100:880–83

Briggs, L. J. 1959. Effect of spin and speed on the lateral deflection of a baseball; and the Magnus effect for smooth spheres. *Am. J. Phys.* 27:589–96

Brown, F. N. M. 1971. See the wind blow. *Dept. Aerosp. Mech. Eng. Rep.*, Univ. Notre Dame, South Bend, Ind.

Cavendish, M. 1982. Balls in flight. *Sci. Now* 1:10–13

Chase, A. 1981. A slice of golf. *Sci. 81* 2(6):90–91

Cochran, A., Stobbs, J. 1968. *Search for the Perfect Swing*, pp. 161–62. Philadelphia/New York: Lippincott.

Daish, C. B. 1972. *The Physics of Ball Games.* London: Engl. Univs. Press. 180 pp.

Davies, J. M. 1949. The aerodynamics of golf balls. *J. Appl. Phys.* 20:821–28

Graham, J. M. R. 1969. The development of the turbulent boundary layer behind a transition strip. *Aeronaut. Res. Counc. Rep. 31492*

Horlock, J. H. 1973. The swing of a cricket ball. In *Mechanics and Sport*, ed. J. L. Bleustein, pp. 293–303. New York: ASME

Hunt, C. 1982. *The aerodynamics of a cricket ball.* BSc dissertation. Dept. Mech. Eng., Univ. Newcastle, Engl.

Imbrosciano, A. 1981. The swing of a cricket ball. *Proj. Rep. 810714*, Newcastle Coll. of Adv. Educ., Newcastle, Austral.

Lyttleton, R. A. 1957. The swing of a cricket ball. *Discovery* 18:186–91

Mehta, R. D., Wood, D. H. 1980. Aerodynamics of the cricket ball. *New Sci.* 87:442–47

Mehta, R. D., Bentley, K., Proudlove, M., Varty, P. 1983. Factors affecting cricket ball swing. *Nature* 303:787–88

Newton, I. 1672. New theory of light and colours. *Philos. Trans. R. Soc. London* 1:678–88

Rayleigh, Lord. 1877. On the irregular flight of a tennis ball. *Messenger of Mathematics* 7:14–16. Reprinted in *Scientific Papers* (Cambridge, 1899) 1:344–46

Sherwin, K., Sproston, J. L. 1982. Aerodynamics of a cricket ball. *Int. J. Mech. Educ.* 10:71–79

Tait, P. G. 1890. Some points in the physics of golf. Part I. *Nature* 42:420–23

Tait, P. G. 1891. Some points in the physics of golf. Part II. *Nature* 44:497–98

Tait, P. G. 1893. Some points in the physics of golf. Part III. *Nature* 48:202–5

Ward, C. W. 1983. *The aerodynamics of a cricket ball.* BSc dissertation. Dept. Mech. Eng., Univ. Newcastle, Engl.

Watts, R. G., Sawyer, E. 1975. Aerodynamics of a knuckleball. *Am. J. Phys.* 43:960–63

Weaver, R. 1976. Comment on "Aerodynamics of a knuckleball." *Am. J. Phys.* 44:1215

Annual Review of Fluid Mechanics
Volume 17, 1985

CONTENTS